M 2022

U.PORTO
FEUP FACULDADE DE ENGENHARIA
UNIVERSIDADE DO PORTO

DEVELOPMENT OF HIERARCHICAL ZEOLITES FOR THE VALORIZATION OF GLYCEROL

CAROLINA JOANA VIEIRA VIVEIROS
MASTER THESIS IN CHEMICAL ENGINEERING
PRESENTED TO THE FACULTY OF ENGINEERING
OF THE UNIVERSITY OF PORTO

Master in Chemical Engineering

Development of hierarchical zeolites for the valorization of glycerol

Master dissertation

of

Carolina Joana Vieira Viveiros

Developed within the course of dissertation

held in

LSRE – LCM – Laboratory of Separation and Reaction Engineering – Laboratory of Catalysis and Materials, part of ALiCE- Associate Laboratory in Chemical Engineering

Supervisor: Drª. Ana Mafalda Ribeiro

July 2022

Acknowledgment

This dissertation is the closing of a chapter in my life, and I wouldn't have achieved this alone. For that reason, I would like to express my gratitude to everyone who contributed to this:

A special thanks to my supervisor, Ana Mafalda Ribeiro, for the availability, assistance, words of encouragement, patience and support provided me throughout this stage. Thanks to my first supervisor Rui Faria, for having proposed this topic and for having started to guide me in this dissertation with all the attention and dedication. Also, thanks to Jonathan for the help provided.

Thanks to Yaidelin and Carla for their availability to use the equipment when needed.

I also want to thank everyone at LSRE-LCM for their willingness to help and good disposition.

Bruno and Isabella, I must thank you for all the dedication, availability shown, and good disposition, even on the worst days you were always there ready to help. I will never forget your companionship. Thank you so much!!

To my friends, thank you so much for friendship. I'm sure you are for life.

A real thank you to all my family that always supported everything to me, and especially to my mom for all the love, the endless support, and that even far away was always present.

And finally, a special thanks to Lima, to whom I owe the completion of this cycle. For the constant presence, for believing in me, for supporting me unconditionally, and for being my shelter.

Professor Ana Mafalda Ribeiro, supervisor of this dissertation is a member of LSRE-LCM - Laboratory of Separation and Reaction Engineering – Laboratory of Catalysis and Materials, financially supported by LA/P/0045/2020 (ALiCE), UIDB/50020/2020 and UIDP/50020/2020 (LSRE-LCM), funded by national funds through FCT/MCTES (PIDDAC).

Abstract

The development of alternative sustainable energy sources to replace non-renewable energies is growing in the industry, such as the biodiesel industry. The growth of biodiesel production is leading to an excess of crude glycerol, as a byproduct of the transesterification reaction. This is economically disadvantageous as it leads to a low economic value of glycerol. Alternatives using glycerol to convert into valuable products have therefore been developed, enhancing the circular economy.

Solketal is one of the routes for glycerol valorization with high economic viability, and it is obtained by the reaction with acetone in a presence of an acidic catalyst. This benign chemical compound can be used as an additive for fuels, improving its properties, and reducing particle emission. However, the low miscibility between glycerol and acetone under normal conditions, and the high viscosity of glycerol, leads to problems in mass transfer which are an impediment to the ketalization reaction. Zeolites, aluminosilicate materials are the most promising catalysts for the synthesis of solketal, but one of the limitations is the access to the active sites, and to get over it, the development of mesoporous structures is made using a demetallation process.

This work aimed to study three acid zeolites: MOR, MFI, and BEA, with different Si/Al ratios as the heterogeneous catalysts to solketal production. These zeolites were submitted to a demetallation process which consists of the removal of atoms from the structure, including desilication and dealumination treatment. Also, the characterization of these zeolites was made with certain techniques which allowed to conclude that the treatments changed the zeolites, mainly in the increase of the mesoporosity. The parent and hierarchical zeolites performance, towards the species involved in the synthesis of solketal, was evaluated in which the MFI zeolite had the most increase in glycerol conversion and selectivity to solketal due to the treatment. To produce solketal, catalyst shaping was done on the hierarchical MFI zeolite and a fixed bed column was packed with these pellets. The synthesis of solketal was carried out and it was verified that the conversion of glycerol to solketal was obtained.

Keywords: solketal, glycerol ketalization, hierarchical zeolites, fixed-bed reactor

Resumo

O desenvolvimento de fontes alternativas de energia sustentável em substituição às energias não renováveis está a crescer na indústria, como é no caso da indústria do biodiesel. O crescimento da produção de biodiesel está a provocar um excedente de glicerol bruto, sendo este o subproduto da reação de transesterificação. Isto é economicamente desvantajoso e faz com que o glicerol tenha baixo valor económico. Como tal, é necessário desenvolver alternativas para converter o glicerol em produtos de alto valor, alternativas estas que têm sido desenvolvidas na indústria, de modo a potencializar a economia circular.

O *solketal* é uma das vias de valorização do glicerol com alta viabilidade económica, e é obtido através da reação com acetona na presença de um catalisador ácido. Este composto benigno pode ser utilizado como um aditivo para os combustíveis, melhorando as propriedades físicas e reduzindo as emissões de partículas. No entanto, a baixa miscibilidade entre o glicerol e a acetona em condições normais, e a alta viscosidade do glicerol, levam a problemas como a baixa transferência de massa que impedem a reação de acetalização. Os zeólitos, aluminossilicatos, são os catalisadores mais promissores para a síntese de *solketal*, contudo uma das uma das limitações o acesso aos sítios ativos, e para superar isso, o desenvolvimento da estrutura mesoporosa é feito a partir do processo de desmetalização.

Este trabalho teve como objetivo o estudo de três zeólitos ácidos: MOR, MFI e BEA com diferentes razões de Si/Al como catalisadores heterogéneos para a produção de solketal. Estes zeólitos foram submetidas a um processo de desmetalização, que inclui o tratamento de desilicação e desaluminação, e consiste na remoção de átomos da estrutura. A caracterização dos zeólitos foi efetuada a partir de determinadas técnicas, de forma a verificar os efeitos dos tratamentos sobre os zeólitos. Foi avaliado ainda o desempenho dos zeólitos originais e modificadas, em relação às espécies envolvidas na síntese de *solketal*, sendo o zeólito MFI o que teve o maior aumento na conversão de glicerol e seletividade de solketal devido ao tratamento. A moldagem em *pellets* foi feita a partir do zeólito MFI tratado (hierárquico) para o empacotamento de uma coluna de leito fixo. A síntese de *solketal* foi realizada e verificou-se que a conversão de glicerol em *solketal* foi obtida.

Palavras-chave: *solketal*, cetalização de glicerol, zeólitos hierárquicos, reator de leito fixo.

Declaration

I hereby declare, under word of honor, that this work is original and that all non-original contributions are indicated, and due reference is given to the author and source

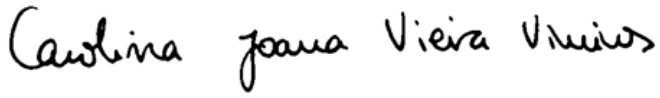

4th July 2022

Index

List of Figures

List of Tables

Notation and Glossary

List of Acronyms

BEA	Structure code for beta zeolite
GC	Glycerol Conversion
GHG	Greenhouse gas
IUPAC	International Union of Pure and Applied Chemistry
IZA	International Zeolite Association
LCA	Lifecycle Assessment
MFI	Structure code for Z-SM5 zeolite
MIP	Mercury intrusion porosimetry
MOR	Structure code for mordenite zeolite
NZE	Net Zero Emissions Scenario
PDA	Pore-directing Agents
SS	Selectivity to Solketal
XRD	X-ray diffraction
Z-SM5	Zeolite Socony Mobil number 5

1 Introduction

1.1 Framing and presentation of the work

The global warming increase and the decline in fossil fuel resources have led to the search and development of energy alternatives to replace non-renewable energies, contributing to the reduction of emissions to the environment. Biofuel production, such as biodiesel, appears as an alternative to fossil fuel usage through the transesterification reaction of vegetable oil or animal fats with methanol, in the presence of a catalyst, favoring the production of glycerol. A surplus of glycerol is generated due to the growth in biodiesel production, reducing the glycerol price. For such, alternatives that use glycerol and convert it into valuable products are being developed.

Glycerol can be transformed into several chemical intermediates, and one of the most promising alternatives for the valorization of this compound is the synthesis of solketal, obtained through the ketalization reaction of glycerol with acetone in the presence of an acid catalysts. This compound can be used as an additive for fuel to increase the octane number and therefore decrease the emissions resulting from the combustion of the fuel, thus improving the properties of biodiesel. The process can be carried out in fixed bed adsorptive reactors using hierarchical zeolites that increase the catalytic capacities of the process. Hierarchical zeolites are prepared through various post-synthesis treatments. These treatments consist of removing atoms from the material's structure, namely from the demetallation process for the material's mesoporosity development.

In this work, three types of zeolites: MOR, MFI, and BEA, were submitted for demetallation treatment, and their catalytic performance was evaluated. The best performing zeolite was shaped into pellets and packed in a column to assess the kinetic activity and conversion for the production of solketal.

1.2 Contribution of the author to the work

The experimental treatment of the zeolites in this work was already defined as well as the analytic method used in the gas chromatograph to determine the conversion and selectivity during the catalytic tests and the solketal production.

However, I was the first in the LSRE-LCM to transform the BEA and MOR structures in hierarchical zeolites as well as to evaluate the catalytic activity of zeolites: MOR, MFI, and BEA. Also, I was the first one to develop a formulation to extrude pellets with the zeolites treated to pack a fixed-bed column and do an experiment.

1.3 Organization of the dissertation

This work is divided into six chapters: Introduction, Context and State of the Art, Material and Methods, Results and Discussion, Conclusions and the Assessments of the work done.

In Chapter 2, Context and State of Art, is summarized the information related biodiesel production as an alternative to fossil fuels with a surplus of glycerol as a primary by-product. Routes for the valorization to glycerol are discussed with focus on solketal, as an additive capable of reducing particulate emission and optimizing the biofuel properties.

Chapter 3, Materials and Methods, contains the information on the selected zeolites, the demetallation process to incorporate a mesoporous structure in the zeolites, the material characterization, and the experimental catalytic tests. Finally, it has a description of the adopted procedure for the shaping process and the experimental process of synthesis of solketal in a fixed bed column.

Chapter 4, Results and Discussion, contains the results of the characterization of the zeolites after the demetallation process as well as the evaluation of the hierarchical zeolite catalytic activity for glycerol conversion and selectivity to solketal. The shaping procedure was investigated, and the optimal formulation of the mixture was defined. The developed pellets were used in a fixed-bed column for the production of solketal, and its potential application was demonstrated.

Chapter 5, Conclusion, summarizes the main conclusion of the experimental results.

Finally, Appendix A and B serve as support to this work.

2 Context and State of the art

2.1 Glycerol

Glycerol, also known as propane-1,2,3-triol, is an organic molecule belonging to the alcohols family and has a density, viscosity, boiling point, and heat of vaporization of about 1.26 g·cm^{-3} (at 20ºC), 1.5 Pa·s, 290 ºC, and 88.12 kJ·mol^{-1}, respectively [1]. It is a viscous liquid, odorless, colorless, low toxicity alcohol, that contains three hydrophilic hydroxyl groups (Figure 1) [2]. These groups are responsible for complete miscibility with water and its highly hygroscopic nature [1]. Due to its physical and chemical properties, it can be used in different fields, especially in the pharmaceuticals, food, cosmetics, and polymer industries [3].

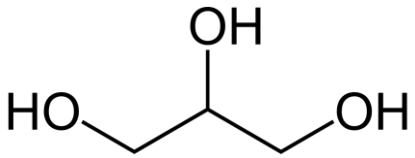

Figure 1. Glycerol chemical structure.

The amount of glycerol available and its high valorization potential justify its selection as a platform molecule, so it is a highly functionalized molecule, that can be incorporated as a raw material to obtain molecules of industrial interest, providing sustainable alternative routes to the traditional ones. Therefore, many processes can make glycerol a valuable by-product, by obtaining a purer product or by chemical reactions, with the most common being thermochemical conversion, oxidation, hydrogenolysis, esterification, biological conversion, aqueous phase, and bioconversion [4].

Glycerol was discovered in 1779 by Scheele, who heated a mixture of litharge and olive oil and extracted it with water. Glycerol occurs naturally in glycerides in all animal and vegetable fats and oils and is recovered, as a by-product when these oils are saponified in the process of manufacturing soap, when the fats are split in the production of fatty acids, or when fats are esterified with methanol in production of methyl esters [1]. In soap manufacture, fat is boiled with caustic soda solution and salt, causing separation into layers of soap, and spent lye, which contains glycerol, water, salt, and excess caustic. These processes are common to produce soap and spent lye. In the production of fatty acids, high-pressure hydrolysis, in which a fat continuously flows upwards through the column, in countercurrent to water, and the fat is split by water into fatty acids and glycerol. The fatty acids formed are used to make soap, reduced to the corresponding fatty alcohol, or marketed as fatty acids [1, 5].

Transesterification of fats with alcohol to produce fatty esters is another source of glycerol, and it is produced through the reaction of vegetable oil or animal fats with methanol, in the presence of an catalyst resulting in the formation of a significant amount of waste glycerol phase [6].

2.2 Biodiesel

The importance of biofuels has been growing due to the increase in global warming, and the decrease in fossil fuels resources has led to the development of alternative and sustainable energy sources to replace non-renewable energies. The transport sector relies heavily on fossil fuels and is one of the largest contributors to the world's greenhouse gas (GHG) and CO_2 emissions hence, this alternative results in a reduction of emissions to the environment. In 2020, the global transport sector emissions were 7.2 Gt CO_2, down from almost 8.5 Gt in 2019, falling by more than 10 % due to restrictions and lockdowns related to COVID-19 [6, 7].

Under the Net Zero Emissions Scenario (NZE), direct CO_2 emissions from fossil fuel used by transport should decrease 8,5 % per year on average between 2020 and 2030 [8]. Furthermore, to reduce the dependence on petroleum-based fuels due to environmental issues, high transport costs, and limited oil reserves, biofuels are attractive as a promising alternative worldwide as a carbon-neutral, sustainable, and renewable source [9, 10].

Biodiesel production is a sustainable, versatile, and environmentally friendly alternative to fossil fuels obtained through the transesterification of animal fats or vegetable oils (triglyceride) with a mono-alcohol, usually methanol, in the presence of a catalyst (Figure 2), which possesses virtually the same characteristics as diesel, and is viewed as an appealing substitute to diesel fuels. Many studies using lifecycle assessment (LCA) demonstrated that biodiesel results in 20-80% fewer greenhouse emissions when compared to petro-diesel [11, 12].

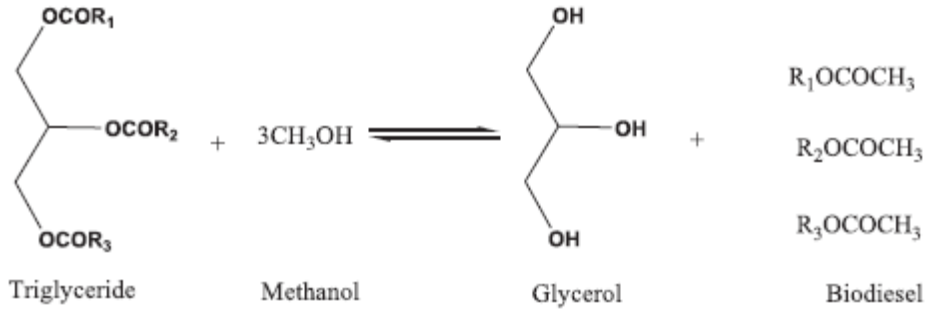

Figure 2. Synthesis of biodiesel and glycerol by the transesterification reaction [3].

The gross growth of the biodiesel market is expected to reach $24,11 billion in 2022. With the increase in biodiesel production comes a growing surplus of glycerol as a primary by-product, since producing 100 l of biodiesel production yields approximately 10 l of glycerol.

Due to biodiesel production increase since the 2000s (Figure 3), this industry became the main producer of crude glycerol, of which 50-80 % is generated from the transesterification process [4, 10, 12-16]. Thus, growth of biodiesel plants and the increased quantities of crude glycerol make a whole world's glycerol production surpass 1400 metric tons (Figure 3) in 2020, and stabilization and a possible decline in biodiesel production are expected in the next decade because of second and third-generation biofuel development and industrial application, with products obtained from non-edible sources[4, 10, 17]. .

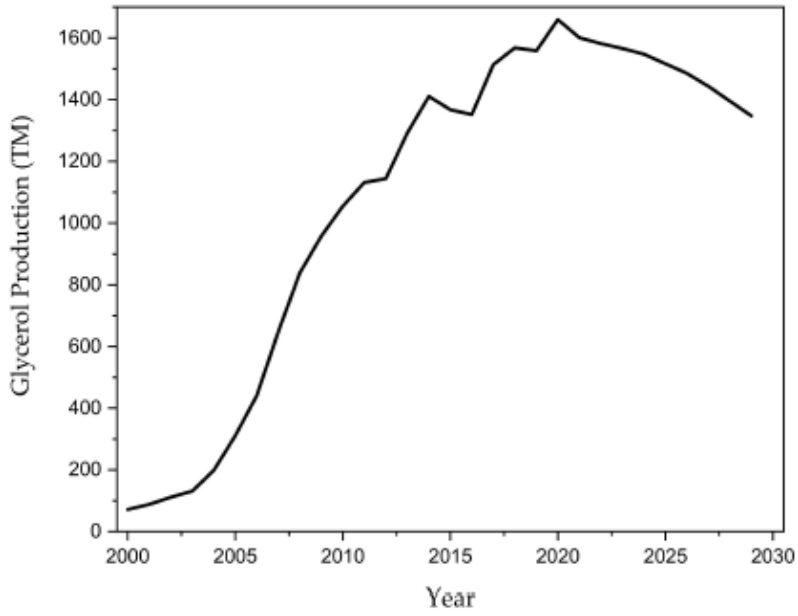

Figure 3. Glycerol production in the biodiesel industry[4].

Nevertheless, the co-production of glycerol in the conventional biodiesel processes is economically disadvantageous for biodiesel plants because the global glycerol production causes an oversupply, significantly reducing the glycerol price [16]. Crude glycerol is contaminated with many chemicals, and the purification procedures to eliminate impurities such as water, methanol, fatty acids, esters, and other compounds, to increase glycerol purity present a limited economical advantage. Additionally, purification procedures to eliminate impurities causes environmental problems because treatment is required before discharge into the atmosphere [10].

For this purpose, alternatives using glycerol as the main feedstock to generate value for many products are important to convert glycerol into valuable products. This is necessary to increase the biodiesel economic viability, and it is possible by transforming the byproduct into higher-value components, from different pathways as thermochemical, catalytic, chemical, and biological [12, 15]. The glycerol valorization is vital to make biodiesel production a more competitive and sustainable alternative for petroleum-based fuels and will also help meet the circular bioeconomy guidelines.

One of the promising procedures for low-value glycerol valorization is the reaction with ketones or aldehydes in the presence of an acidic catalyst to produce acetals or ketals, with water as the by-product [17]. This has significant potential when applied as fuel additives and biofuels. Among ethers and esters, glycerol acetals and ketals constitute excellent diesel and biodiesel blend compounds, which improve the oxidation stability, enhance the octane number, and reduce particle emission, and gum formation [3, 13, 18].

2.2.1 Solketal: an additive for biodiesel

Solketal (2,2-Dimethyl-4-hydroxymethyl-1,3-dioxane) is one of the recurrent glycerol valorization routes. It is obtained from the ketalization reaction of glycerol with ketones (Figure 4) in the presence of an acidic catalyst. Its isomer (2,2-dimethyl-1,3-dioxan-5-ol), which is thermodynamically less stable than the solketal molecule, is also produced but at a much lower extent. It is a condensation product that is oily, colorless, liquid, and a potential fuel additive capable of reducing particulate emission and optimizing the octane number in fuels [3, 19]. It has a density, viscosity, boiling point, and flash points of about 1.06 $g \cdot cm^{-3}$ (at 20ºC), 0.011 Pa.s, 190 ºC, and 80 $kJ \cdot mol^{-1}$, respectively.

Furthermore, it has been widely used in industry as a versatile solvent for medical applications and a plasticizer in the polymer industry, a base for the surfactants, and suspending agent in pharmaceutical preparations [3, 20]. This route of valorization is economically promising as the selling price of solketal is around US$3,000/ton, while crude glycerol is between US$210–390/ton, making production more profitable [21].

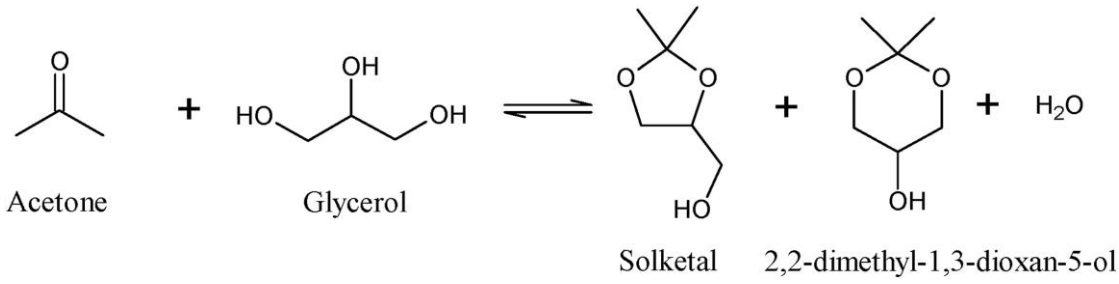

Figure 4. Glycerol and acetone reaction to produce Solketal[22].

Ketalization reaction of glycerol with ketones to produce ketal over an acidic catalyst is a reversible reaction (Figure 5). The major steps are nucleophilic attack, water elimination (dehydration), and proton migration. In the first step the glycerol hydroxyl group attacks the acetone carbonyl carbon atom to form the intermediate hemiketal [12, 23]. The electronic and steric factors strongly affect the ketal formation, and the reaction mixture is strongly acidic to allow the protonation of ketal to enable cationic intermediate stabilization. In the second step,

water is eliminated, and a carbocation is formed. In the third step the secondary hydroxyl group from glycerol attacks the carbonyl carbon atom, releasing its proton and forming a five-membered ring species, solketal. Cyclic ketals are synthesized by the reaction with a polyol, which in this case is glycerol in the presence of the ketones and produce 1,3-dioxolane(5 membered ring) and not a 1,3-dioxane (6 membered ring) structures because of steric blockages from positions 4 and 6 of the molecule by the radicals and hydrogen atoms [12, 18, 23].

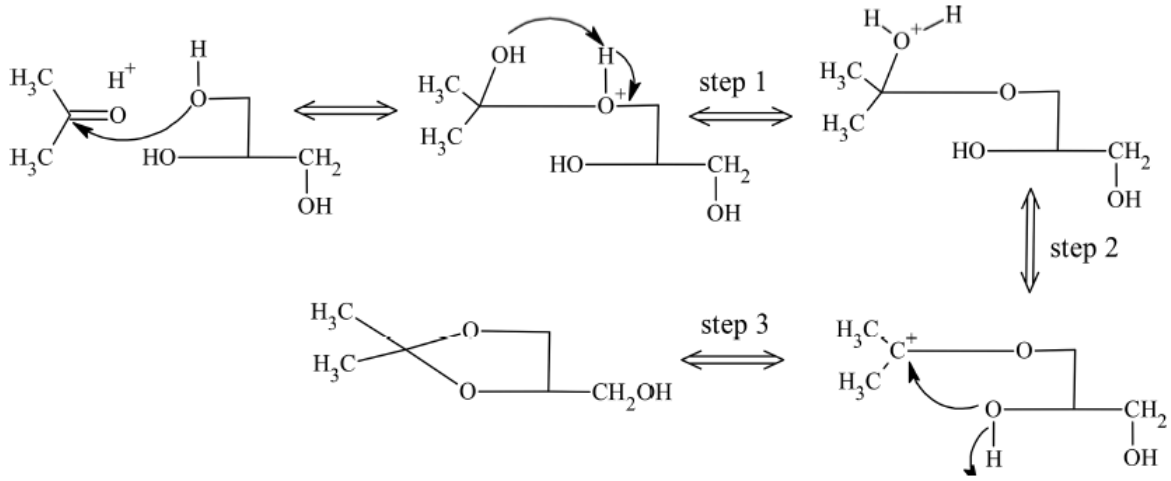

Figure 5. Mechanism of glycerol ketalization with acetone [23].

The low miscibility between glycerol with acetone at normal conditions (25ºC and 1 atm), in which only 5 wt% of glycerol is soluble in acetone, constitutes an enormous disadvantage for the synthesis of solketal. Moreover, the major issue in the ketalization reaction is the formation of the byproduct water, which creates a thermodynamic and kinetic impediment for high glycerol conversion to solketal, which is catalyzed by acid sites and has a low equilibrium constant [3, 22]. On the other hand, mass transfer problems are related to the high viscosity of glycerol.

It is essential to obtain a high glycerol conversion to increase the formation of solketal, and there have been studies searching for a stable, easily accessible, and active catalyst for the ketalization reaction using traditional liquid inorganic acids, which involves problems such as products separation and the utilization of spent catalysts beyond being environmentally unaccepted [3, 24, 25]. Among solid acid catalysts used for the synthesis of solketal, such as modified mesostructured silica, or acidic resins, zeolites are the most promising.

Most studies on solketal synthesis were performed with batch reactors with catalysts, but the limitation of an extended reaction time, poor mass transfer, low efficiency, and the enormous labor requirements make this process disadvantageous. To avoid these problems, the continuous-flow process using catalysts proved an improved efficiency and provided higher heating performance and mass transfer efficiencies besides being more environmentally and

economically advantageous [16, 24, 25]. Furthermore, the advantage of continuous operation is the possibility of scaling up at the industrial level.

2.2.2 Acidic catalyst: Hierarchical Zeolites

Zeolites are an important class of inorganic microporous crystalline structures. They are aluminosilicate materials, with a three-dimensional framework, composed of tetrahedral units of alumina (AlO_4^{5-}) and silica (SiO_4^{4-}) by sharing their vertex oxygen atoms[26]. A wide range of applications in the petrochemical industry results in shape selectivity, strong acidity, high stability, easy regeneration, low price, pore size distribution, and crystallite size. These properties make zeolites an indispensable material for catalysis, separation/adsorption, and ion-exchange processes [25-29].

However, the framework of zeolites possesses pores with diameters less than 2 nm that are classified as micropores, which hinders the diffusion of the bulky reactants/products of the ketalization reaction. So, one of the major limitations of the use of zeolites as catalysts/adsorbents is the limited access to the active sites within the individual crystals. An alternative to minimize the diffusion limitation is the development of hierarchical zeolites that integrate porosities of multiple levels, creating a mesoporous structure with high mesopore surface area [26, 30, 31].

The preparation of the hierarchical zeolites into a mesoporous structure is categorized into two approaches: *in situ* or pre-synthesis and post-synthesis. The pre-synthesis modification consists of exfoliation, pillaring, silanization, solid zeolitization, and templating. In this case, the approach concerns the post-treatment to introduce a hierarchical structure into zeolites, including demetallation involving removal of Al or Si atoms from the zeolite framework, which incorporates mesoporosity in the length scale of 2-50 nm, comprising dealumination and desilication [26, 31].

Demetallation comprises the dealumination and/or desilication process, by the zeolite treatment by the selective chemical extraction of one constituent from the native zeolite framework (Figure 6). The extracting process requires the usage of strong acids for the aluminum atoms (dealumination) and bases for the silicon removal(desilication), respectively causing the formation of mesoporosity [31-33]. The extraction of silicon atoms (desilication) from zeolite framework occurs in alkaline medium, and as a result of this extract, Si-O-Si splitting occurs [26]. Thus, resultant materials exhibit a decrease in the Si/Al and an increase in the ion exchange capacity [32, 34].

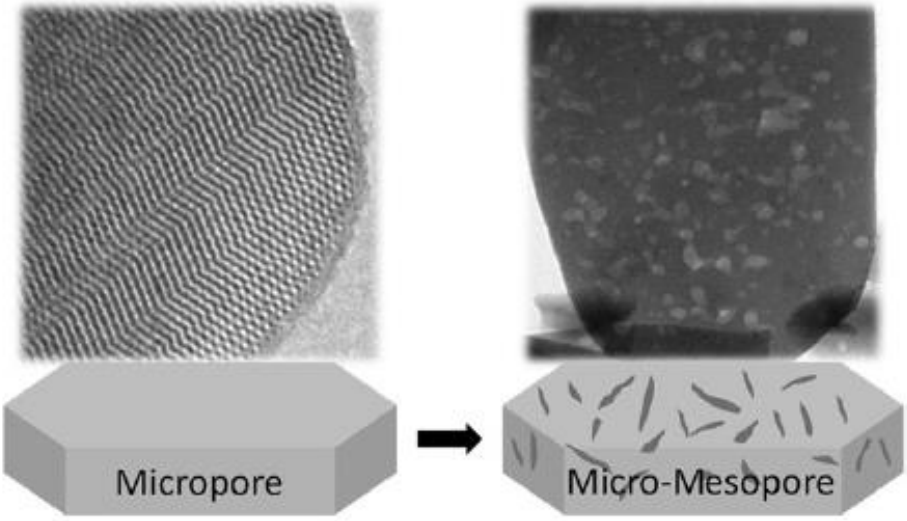

Figure 6. Schematic transformation by demetallation process of a zeolite into a hierarchical micro-mesoporous material [28].

To remove the aluminum atoms, in dealumination, the hydrolysis of Al-O-Si bonds is achieved by a heat steam treatment followed by calcination and acid leaching. The increased Lewis and Bronsted acid sites and stable crystalline structure occur due to heat steam treatment, in which the breakdown of the bonds makes a loss of aluminum facilitate the movement of less stable silicon to the lost sites originating a formation of silanol-rich domains. In addition, the acid leaching is essential to remove debris that are deposited on the zeolite surface or inside pores. The remove aluminum from the zeolite structure increases the Si/Al ratio [32-34].

3 Materials and Methods

3.1 Hierarchical zeolites

MOR (Clariant©, Si/Al =20,6; denoted as MOR P), MFI (Zeolyst, Si/Al =23; denoted as MFI P), and BEA (Clariant©, Si/Al=35; denoted as BEA P) were used as parent (P) zeolites submitted a demetallation process, comprising dealumination and desilication treatment, with different SiO_2/Al_2O_3 ratios. Zeolites were provided in powder which MFI comes in the ammonium form, and MOR and BEA in sodium form. The framework of each zeolite is shown in Figure 7.

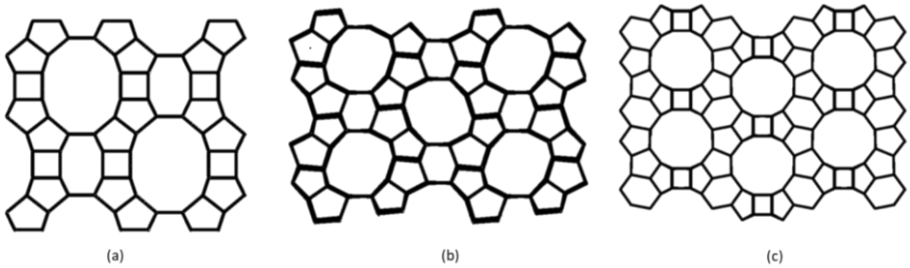

Figure 7. Zeolite framework of (a) MOR, (b) MFI and (c) BEA. Adapted from [35].

Zeolites are aluminosilicates with a three-dimensional framework with intersecting channels (Figure 8). MOR, MFI, and BEA are composed of 12-rings straight interconnected to 8-ring sinusoidal channels; 10-rings straight interconnected to 10-rings sinusoidal channels; and 12-rings straight which are interconnected to 12-rings sinusoidal channels, respectively. Table 1 shows a comparison of MOR, MFI, and BEA zeolites for pore size and acidity characteristics [35].

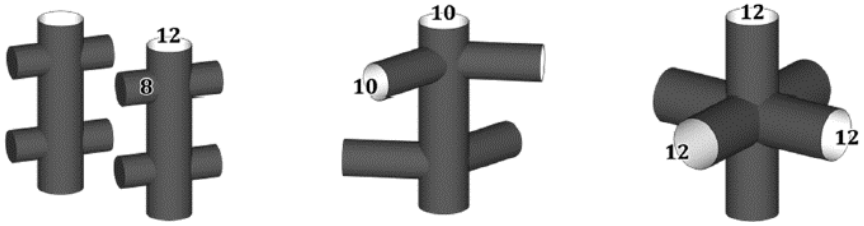

Figure 8. Schematic drawing of channels on three-dimensional network of MOR, MFI, and BEA, respectively [36].

Table 1. Characteristics of MOR, MFI, and BEA [24].

	MOR	**MFI**	**BEA**
Pore Size	6.7 - 7 Å	5.1-5.5 Å	6.1- 6.7 Å
Pores	Large	Medium	Large
Acidity	Strong	Strong	Strong

3.1.1 Zeolite modification methods

The procedure of Castro, B. (Thesis, 2020), for the treatments of zeolites was followed, which includes alkaline treatment, ion exchange, and acid treatment in the experimental setup outlined in Figure 9 *[37]*. The respective applied treatments are represented in Table 2, and the zeolites after the demetallation process are marked as follows: MOR(H), MFI(H), and BEA(H).

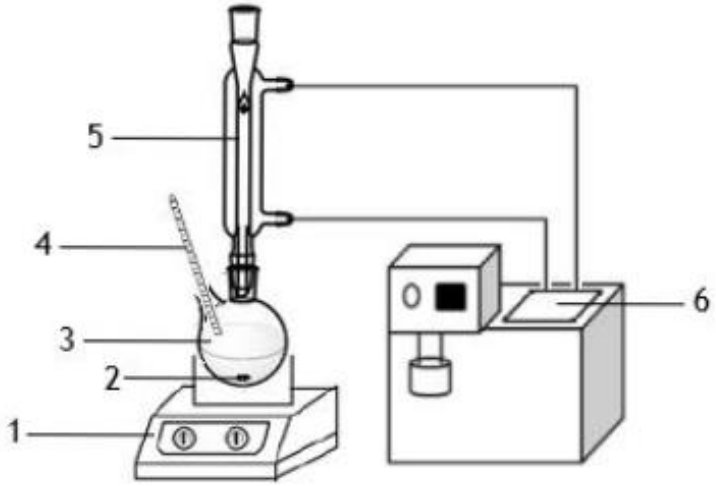

Figure 9. Experimental setup. 1. Heating plate. 2. Magnetic stirrer. 3. Volumetric flask. 4. Thermometer. 5. Condenser. 6. Thermostatic bath [37].

Table 2. List of zeolites and applied treatments.

Zeolite	SiO_2/Al_2O_3	Applied treatments			
		Alkaline treatment		Ion exchange	Acid treatment
		Base Concentration	PDA Concentration		
MOR P	20.6	0.5 M NaOH	0.05 M TPABr	0.1 M NH_4NO_3	0.5 M HCl
MFI P	23				
BEA P	35				

3.1.1.1 Alkaline treatment - Desilication Treatment

The catalysts samples (5 g of zeolite) were submitted to an alkaline treatment to silicon removal. A solution with a concentration of 0.5 M of sodium hydroxide (NaOH) and 0.05 M of tetrapropylammonium bromide (TPABr) (2.0 g of NaOH solid and 1.33 g of TPABr) in 100 ml of deionized water was prepared. The use of the pore-directing agents (PDA) as a pore regulator,

TPABr, is to protect the surface against the alkaline treatment, forcing the attack on inner pores with the NaOH.

The alkaline solution was heated at 353 K and then, the zeolite was added. This treatment took place for 1 h, under reflux, with the magnetic stirring at 500 rpm to keep the mixture homogenous, and the temperature was controlled by the condenser using water from the thermostatic bath. The samples of each zeolite obtained were centrifuged and washed with deionized water until reaching a neutral pH which was measured with indicator strips and dried overnight at 353 K.

3.1.1.2 Conversion into protonic form (Ion-exchange)

After drying, the samples were converted to the protonic form through three consecutive exchanges using a 0.1 M NH_4NO_3 solution, which was prepared from 0.8 g of the respective compound and dissolved in 100 mL of deionized water, with each exchange lasting 1 hour at 353 K, followed by centrifugation.

The samples were submitted to an intensive washing with NH_4NO_3, after this conversion, to ensure the removal of volatile/harmful products in the environment, such as NOx, which can form during the drying/calcination step. Thereafter, the samples were pre-dried at 353 K and then kept at 393 K overnight to be calcined at 823 K for 4 h to obtain the protonated forms.

3.1.1.3 Acid treatment- Dealumination Treatment

After ion exchange, the samples were treated with a 0.5 M HCl solution, prepared from a 12 M solution, diluting 4.2 mL in a 100 mL volumetric flask, for 2 h at 353 K. The samples were washed and centrifuged with deionized water until neutral pH and dried overnight at 353 K. This treatment was applied to effective removal of aluminum debris that could have formed.

3.1.2 Catalyst characterization

The treated zeolite catalysts were characterized for knowledge of the physical properties and the structural relationships during the catalytic modification process, with a combination of the techniques of spectroscopic characterization as X-ray diffraction, N_2 adsorption, and mercury intrusion porosimetry are used for catalyst characterization.

3.1.2.1 X-Ray diffraction (XRD)

X-ray diffraction is a non-destructive technique for characterizing the crystallinity, structures, phases, and other structural parameters of a material. XRD works on the principle

of Bragg's equation, which results from a process in which X-ray beam incidence and scattering on material by the electrons of atoms present in the material without changing the wavelength, which corresponds to the crystallographic planes of material. The peak intensities are determined by the distribution of atoms within the lattice [38, 39].

XRD was performed using Empyrean diffractometer from Panalytical, at the University of Málaga at an accelerating voltage of 45 kV and an emission current of 40 mA with Cu $K_{\alpha 1}$ (λ=1.5405980 Å) radiation.

3.1.2.2 N_2 adsorption

The liquid nitrogen adsorption at a temperature of 77 K, is a non-destructive technique to characterize the porous structure of the material and measure the specific surface area, volume, and pore size distribution of materials, through the nitrogen adsorption/desorption isotherms of material, which is the relationship between the pressure and adsorption amount at a constant temperature [40].

N_2 adsorption/desorption isotherms at 77 K were performed using a Micromeritics ASAP 2420 (manometric adsorption system), at Laboratorio de Sólidos Porosos, Servicios Centrales de Apoyo a la Investigación (SCAI) from University of Málaga.

3.1.2.3 Mercury intrusion porosimetry (MIP)

Mercury intrusion porosimetry is a destructive technique for determining the pore size distribution, porosity, volume of pores, and surface area. This technique involves the mechanism of transporting mercury, a non-wetting liquid, through the capillaries under specific pressure to fill voids in the surface of a sample, using the Washburn equation to obtain the pore size from the applied pressure [41].

MIP was measured using a Micromeritics AutoPore IV 9500 Series (USA), at Laboratorio de Sólidos Porosos, Servicios Centrales de Apoyo a la Investigación (SCAI) from University of Malaga.

3.2 Catalytic activity tests for glycerol ketalization reaction

The catalytic performance of the prepared hierarchical zeolites was tested to choose the best catalyst/adsorbent for the process of ketalization of glycerol with acetone to produce solketal. The chemicals used in this work are acetone (100%, VWR®), glycerol (99,5%, VWR®), and the solvent ethanol (99,9%, Merk®). The mixtures are composed of the stoichiometric ratio

1:1 of acetone and glycerol diluted in 50 % of solvent (molar basis), in 250 mL glass vessels, loaded with 1.0 wt% of each parent and hierarchical zeolite as catalyst considering the mass of the system (mass of reactants plus the mass of the solvent). The batch reaction was carried out at 323 K a 250 rpm, in an incubator shaker SI300R. Additionally, the reaction time was set to 8 h and samples of each mixture were collected after 3 h and 8 h during the reaction experiments.

The samples were analyzed in a gas chromatograph (SHIMADZU GC) equipped with a flame ionization detector (FID) in triplicate and using a capillary column BPX (length 30 m, inner diameter 0.35 mm, and film thickness 0.25 μm) in which helium was used as the carrier gas at a flow rate 25 ml·min^{-1}. The linear velocity was set at 30 cm·s^{-1} and a split ratio of 120. The sample injection volume was 1 μL at 573 K. The oven temperature program started at 318 K rising to 333 K in 15 min and then to 423 K at 35 K·min^{-1}. The temperature of 423 K was kept for 1.5 min, and finally, another temperature increases to 483 K at 30 K·min^{-1} was done. Propan-1-ol was used as a washing solvent.

The catalytic activity is related to glycerol conversion (denoted as GC) which is the amount of converted glycerol divided by the amount of glycerol before reaction, and the selectivity to solketal (denoted as SS) is the amount of solketal formed divided by the amount of reacted glycerol, expressed in % according to Equations (1) and (2).

$$Glycerol\ Conversion = \frac{mol\ of\ glycerol\ converted}{initial\ mol\ of\ glycerol} \times 100 \quad (1)$$

$$Selectivity\ to\ Solketal = \frac{mol\ of\ solketal\ formed}{mol\ of\ glycerol\ converted} \times 100 \quad (2)$$

3.3 Catalyst Shaping

As the process of synthesis of solketal will be performed in a fixed-bed reactor, the use of powder hierarchical zeolite is not possible since it has low mechanical strength, which can cause the formation of fines that can cause damage to the equipment. On the other hand, very small particles can cause a high-pressure drop. The material must be formulated into macroscopic shapes as pellets to be implemented industrially.

To reduce these problems, zeolite shaping processes are necessary, which requires the addition of binders. The binders improve the interparticle crosslinking at temperatures sufficiently low to avoid damage to the catalytically active material, conferring hardness to the extrudates. The most commonly used binders in industrial catalysts are clays (aluminosilicates), amorphous aluminophosphate, alumina, silica, and titania. Generally, the binder must be added

in amounts greater than 20% by weight to reach the desired mechanical strength, forming a homogeneous mixture in the presence of a solvent [42].

However, binders can be responsible for negative effects like blocking micropores and active sites or incorporating other atoms in the zeolitic framework. Also, the high-pressure extrusion process can alter the material's physicochemical properties if the pore size is too large, like mesoporous materials, or if the framework is fragile [42, 43].

In order to produce shaped catalytic materials to pack the fixed-bed column, Caleva Multi Lab Extruder (Figure 10) was used. The hierarchical zeolite shaping process involves the mixing of solid materials (Figure 10a): powder zeolite, binder, and water; extrusion of the mixture (Figure 10b) through a die to form a determinate-shape particles; and spheronization (Figure 10c) in which the shaped particles are broken into uniform lengths to a specific shape.

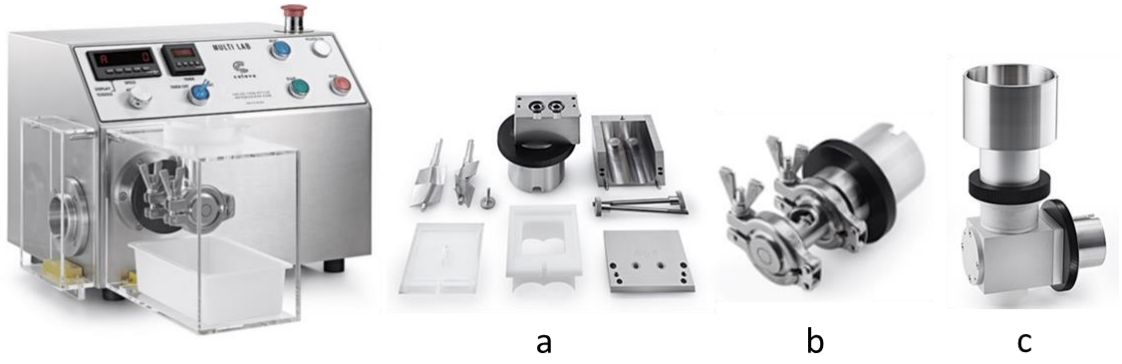

Figure 10. Caleva Multi Lab Extruder and the pieces of equipment: (a) mixing chamber, (b) extruder, and (c) spheronizer. Adapted from [44].

Parent and hierarchical zeolites of the type selected after the catalytic tests were used to prepare the pellets. The zeolites powder was mixed with 30% of binder, an aluminum oxide nanopowder (99%, Alfa Aesar), known as alumina, to form a homogeneous mixture in the presence of ultrapure water. The amount of solvent used in the formulation was evaluated, firstly in the parent zeolite to know the necessary amount of ultrapure water for the mixture and next in hierarchical zeolite prepared in the treatment.

Figure 11. Die for extrusion.

The mixing operation conditions were set at a velocity of the mixture of 80 rpm for a period of 30 min, during which water was added, drop by drop, to obtain a homogenous mixture. After the preparation of the mixture, it was added to the extruder feed tube with the velocity of extrusion set at 60 rpm. To form the pellets the mixtures passed through a perforated die with 2 mm diameter holes (Figure 11). The particles formed after extrusion were placed in the spheronizer, set at a velocity high enough to have a roping-like movement of the pellets. Thereafter, the pellets were pre-dried at 353 K and then kept at 393 K overnight to be calcined at 823 K for 4 h.

3.4 Solketal production in a fixed bed column

In order to evaluate the kinetic activity and conversion of the prepared pellets for solketal production, an experiment was done in a fixed-bed reactor, packed with hierarchical zeolites previously treated and shaped.

The experiment was performed in a jacketed fixed-bed column (length: 11.8 cm; diameter: 1 cm) packed approximately with 4 g of the hierarchical zeolite pellets. A high-pressure liquid chromatographic pump (HPLC) was used, and the temperature of the system was kept at 323K by a thermostatic bath. The setup also comprised an injection valve at the inlet of the fixed bed and a sampling valve at its outlet. The fixed bed was firstly fed with ethanol to saturate the column.

The feed solution is composed of a ternary mixture. The reactants at a stoichiometric molar ratio of 1:1 of acetone (99 %, VWR®) and glycerol (99,5 %, VWR®) and a solvent, ethanol (99,9%, Merk®), present at 50 % in molar basis. The experimental setup is represented in Figure 12.

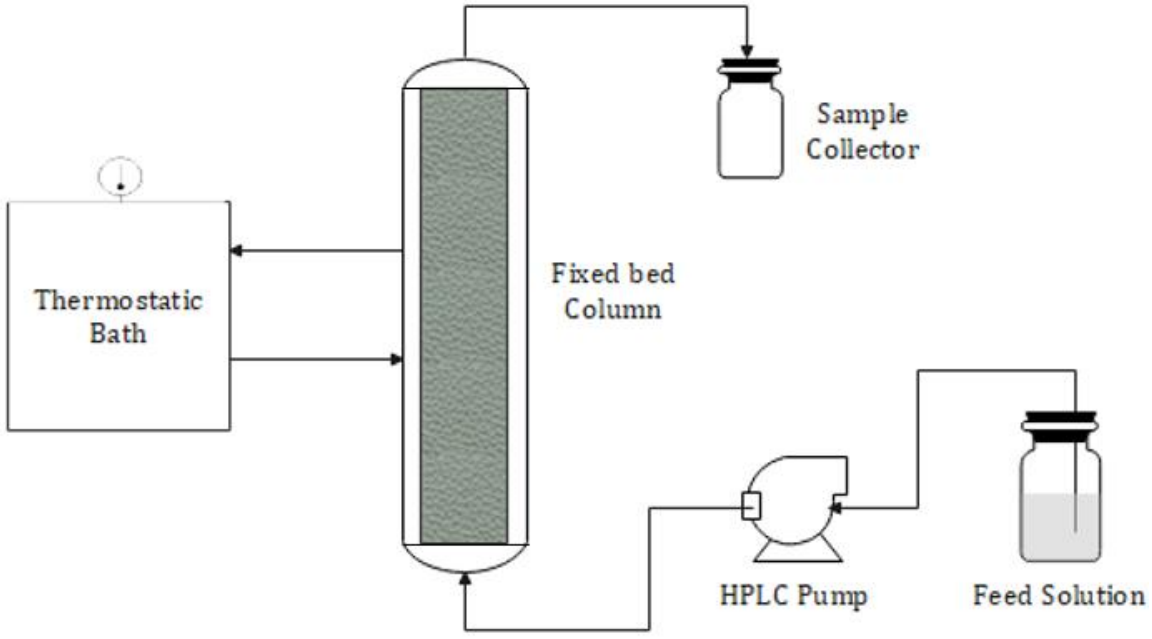

Figure 12. Experimental setup for solketal production in a fixed bed column.

The feed stream flow rate was 0.38 $mL \cdot min^{-1}$. The samples at the column outlet were collected and analyzed in a gas chromatograph (Automatic Liquid Sampler, Dani Master GC). The gas chromatograph was equipped with a flame ionization detector (FID) and a thermal conductivity detector, in which the samples were analyzed in duplicate. The compounds were separated on a silica capillary column PoraBondQ (length 25 m, inner diameter 0.53 mm, and film thickness 0.10 μm) and helium N50 was used as the carrier gas at a flow rate of 8 $mL \cdot min^{-1}$. The linear velocity was set to 40 $cm \cdot s^{-1}$ and a split ratio of 20 was employed. The sample injection volume was 1 μL. The temperature of the injector and of the detectors was set to 573 K, and the column temperature program started at 423 K, increasing 5 $K \cdot min^{-1}$ until 453 K, then increasing at 10 $K \cdot min^{-1}$ until 573 K and holding at this temperature for 2 min. Methanol was used as a washing solvent.

4 Results and discussion

4.1 Catalyst Characterization

4.1.1 X-Ray diffraction (XRD)

The XRD results of parent and hierarchical zeolites of MOR, MFI, and BEA structures are represented in Figures 13, 14, and 15, respectively. Standard samples were used, in which data were taken from the IZA Database that corresponds to the standard of each of the zeolites.

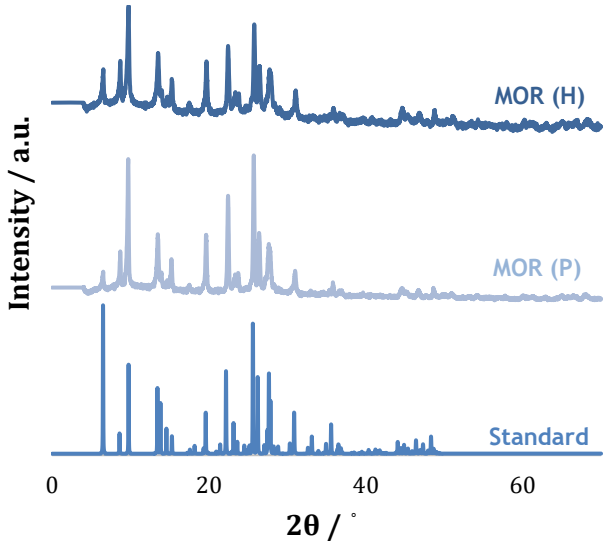

Figure 13. XRD patterns of MOR parent and hierarchical zeolite.

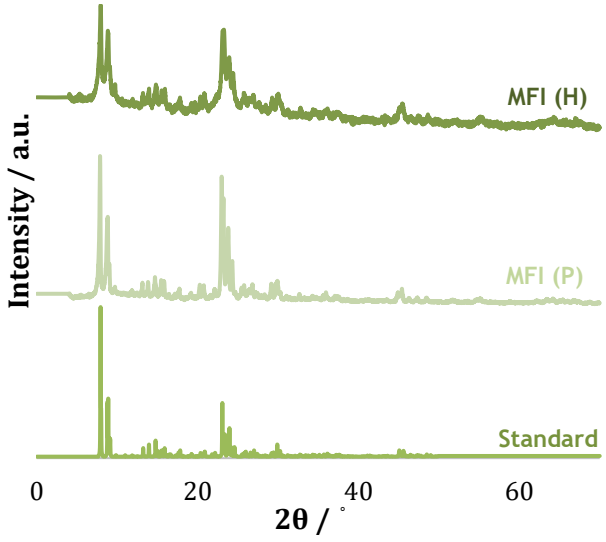

Figure 14. XRD patterns of MFI parent and hierarchical zeolite.

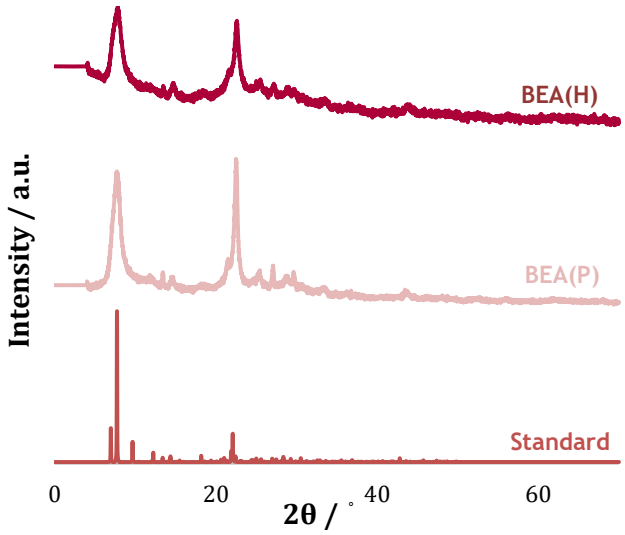

Figure 15. XRD patterns of BEA parent and hierarchical zeolite.

The results of each XRD spectrum shows that all parent and hierarchical zeolites correspond to the structures studied. Besides, the proper structure of zeolite samples has been preserved after the demetallation process which can be explained by the fact that there was no significant change in crystallinity between the hierarchical and standard samples as the XRD spectra displayed similar characteristic diffraction peaks without additional ones. However, the intensity of the characteristic diffraction peaks is different.

4.1.2 N_2 adsorption

Adsorption equilibrium isotherms of nitrogen at 77 K of the samples of parent and hierarchical zeolites are represented in Figures 16, 17, and 18. The assessment is based on the IUPAC isotherm classification.

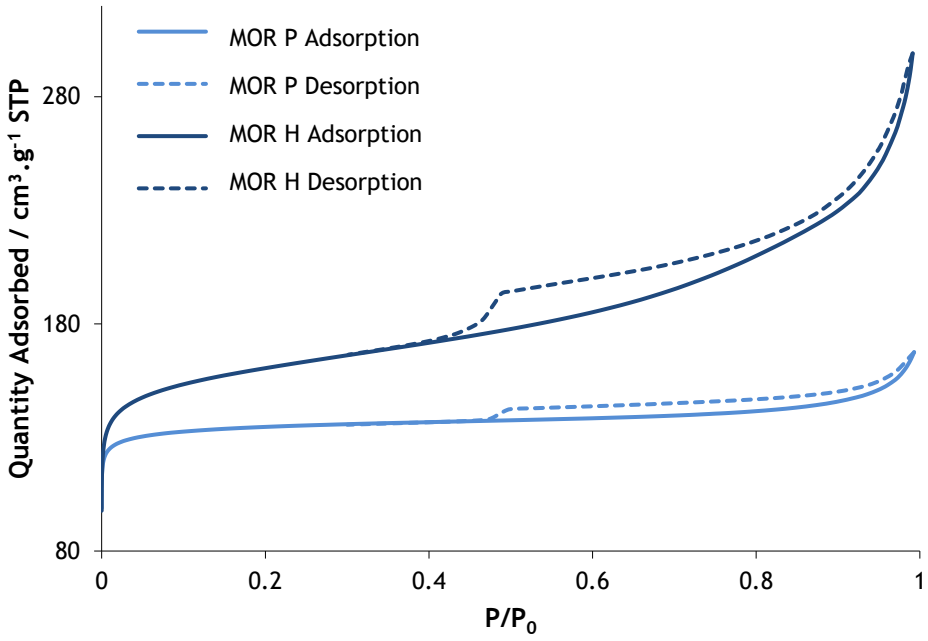

Figure 16. N_2 adsorption//desorption isotherms of the MOR parent and hierarchical.

As shown in Figure 16, the isotherms of MOR parent and hierarchical zeolites were characterized as the type IV isotherm typically found in materials with mesopores. The formation of a structure with a higher volume of mesopores is verified by the increase of the adsorbed amount of N_2, compared to the MOR (P). Moreover, for lower pressures there is a sharp increase in the amount adsorbed which indicates the presence of micropores.

The increase in the hysteresis loop at P/P_0 in the range of 0.42-0.8, classified as an H3 type, which is typically found in materials with wedge-shaped pores [45]. Otherwise, the treatments resulted in an increase in the surface area and mesopore volume (Table 3) for MOR (H) indicating a formation of framework mesoporosity during the treatment processes.

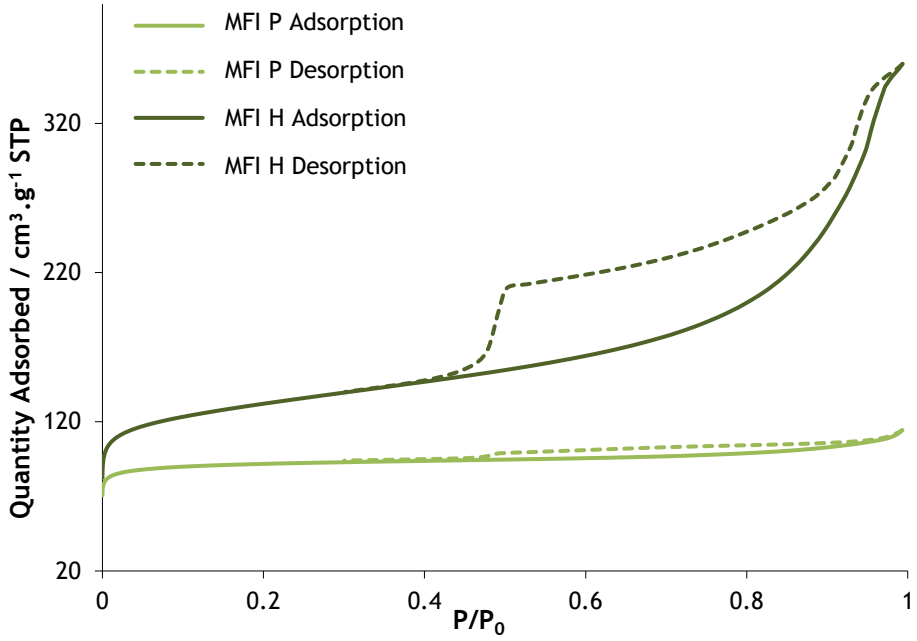

Figure 17. N_2 adsorption/desorption isotherms of the MFI parent and hierarchical.

In the same way, the isotherms of MFI parent and hierarchical zeolites were characterized as the type IV isotherm (Figure 17) typically found in materials with mesopores, whereas for lower pressures the existence of a sharp increase in the amount adsorbed indicates the presence of micropores. The increase in the hysteresis loop, between P/P_0 0.44-0.8, is noticeable in MFI (H) and is classified as an H3 type, which is found in materials with wedge-shaped pores [45]. Besides, the increase in the surface area as noted in MFI(H) is related to the formation of framework mesoporosity and by the growth of total porosity (Table 4) during the treatments.

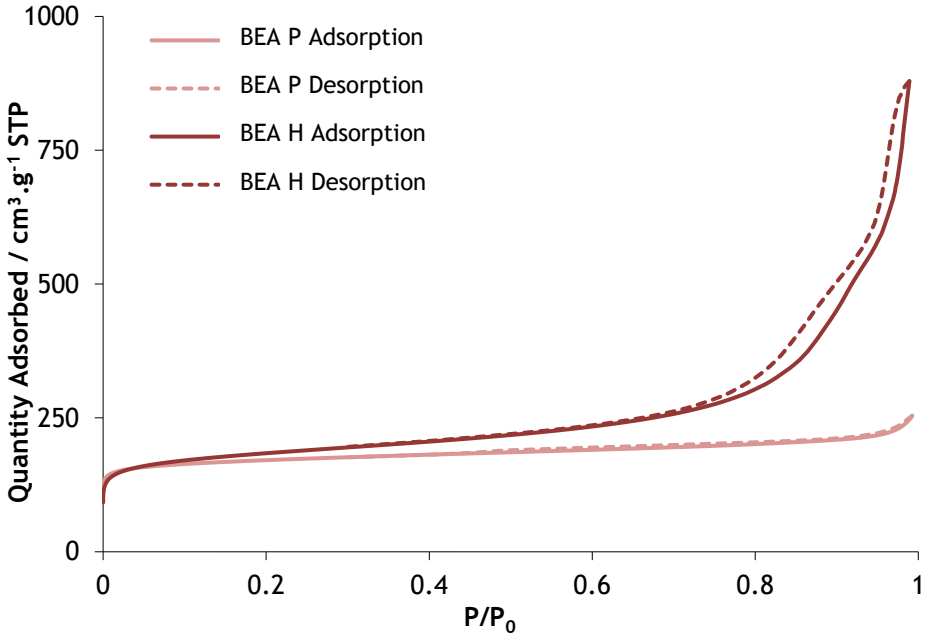

Figure 18. N_2 adsorption/desorption isotherms of the BEA parent and hierarchical.

The isotherms of BEA zeolites exhibit the type IV isotherm (Figure 18) for higher pressures, characteristic of mesoporous materials, while for lower pressures a sharp increase in the amount adsorbed indicates the presence of micropores. The hysteresis loop is categorized as an H3 type which represents the formation of wedge-shaped pores, and a superb increase of the adsorbed amount of N_2 is visible due to the increase of mesoporosity [45]. There was a large increase in the volume of mesopores in BEA (H) (Table 3), demonstrating the effectiveness of the treatment in the formation of mesopores.

Table 3 shows the results obtained by adsorption equilibrium isotherms of nitrogen of the parent and hierarchical zeolites.

Table 3. Characterization of the parent and hierarchicals zeolites.

Sample	Langmuir Surface area / $m^2 \cdot g^{-1}$	Micropore area[a] / $m^2 \cdot g^{-1}$	Micropore volume[a] /$cm^3 \cdot g^{-1}$	Mesopore volume[b] / $cm^3 \cdot g^{-1}$
MOR P	595	579	0.2022	0.0390
MOR H	732	609	0.1955	0.206
MFI P	408	391	0.1354	0.0320
MFI H	618	459	0.1364	0.442
BEA P	779	693	0.2318	0.107
BEA H	868	612	0.1725	0.797

The fact that MFI(P) exhibits a medium pore size framework, and MOR(P) and BEA(P) present a large pore size structure (Table 1), had some influence on the results. The zeolites with larger pores had a higher volume adsorbed in a low/high pressure comparatively to medium size pores. When subjected to a demetallation treatment, an increase in adsorbed volume was visible mainly in MFI (H) and BEA (H).

For all hierarchical zeolites, the external surface area and mesoporous volume increased as shown in Table 3, further demonstrating the effectiveness of the treatment in the formation of mesopores. However, the significant impact of the treatment in MFI (P) on the formation of the mesoporous structure was more evidently by the isotherms represented in Figure 17, with a large increase in adsorbed volume.

[a] Determined by the t-plot method

[b] Determined by the BJH method for the desorption curve

4.1.3 Mercury intrusion porosimetry (MIP)

Mercury intrusion porosity was performed to evaluate the pore size distribution in the range of mesoporosity (2-50 nm) of the samples of parent and hierarchical zeolite. The results obtained are represented in Figures 19, 20, and 21.

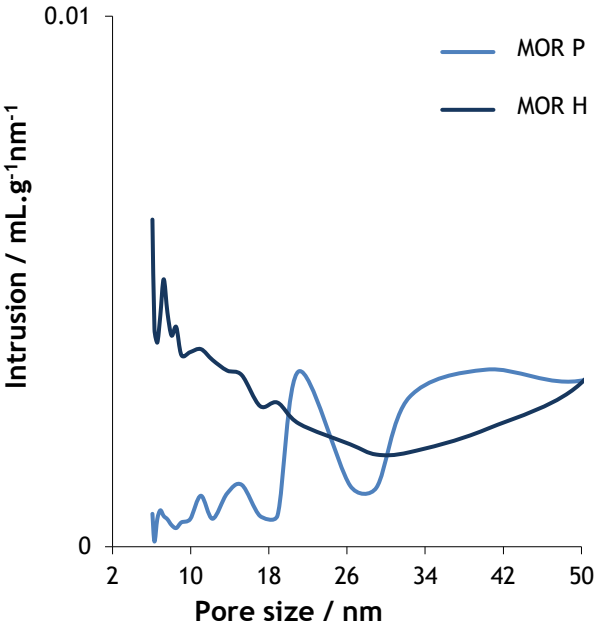

Figure 19. Pore size distribution of the MOR parent and hierarchical.

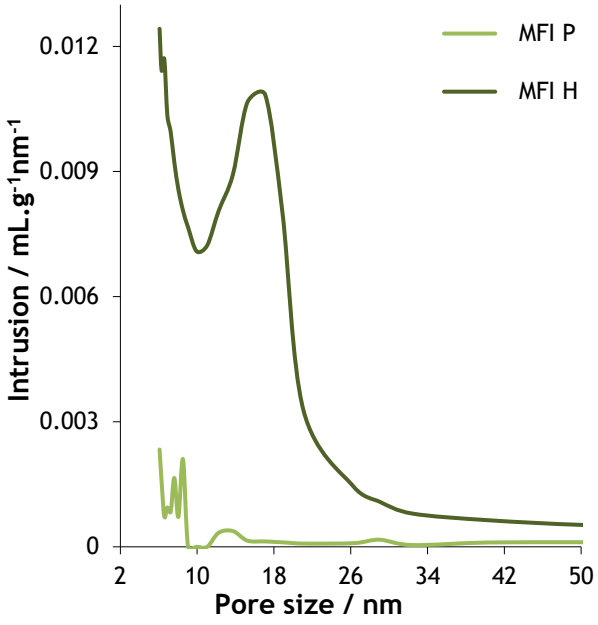

Figure 20. Pore size distribution of the MFI parent and hierarchical.

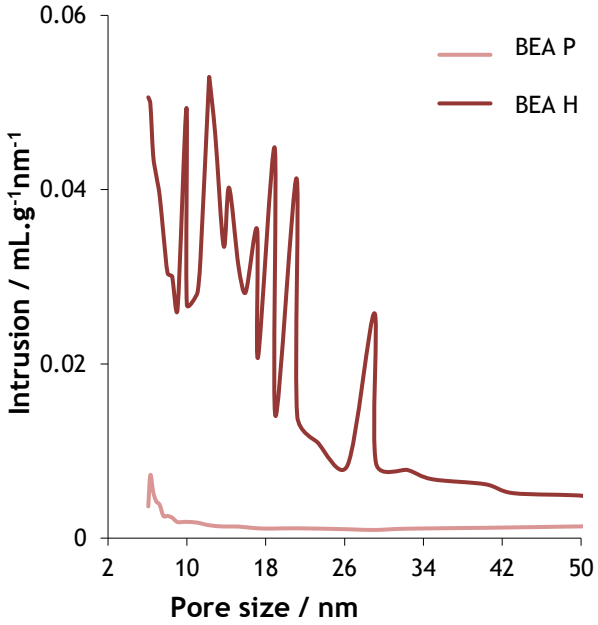

Figure 21. Pore size distribution of the BEA parent and hierarchical.

The results obtained demonstrate that the treatments influenced the increase in mesoporosity, in which there is the formation of a greater amount of small width mesopores.

The use of a PDA in the alkaline treatment can interfere with the results, given the formation of a possibly rough surface, and mercury presents difficulties in measuring volumes accurately in these areas. The distribution of MOR (H) pores was changed after the treatments with the formation of pores mostly with sizes between 6 and 21 nm (Figure 19). Otherwise, the pore distribution of MFI (P) exhibited a pronounced impact due to the treatment, in which there was a significant increase in the amount of pores in a range of 6-18 nm when compared to MFI(P) (Figure 20). Lastly, the distribution of pores in BEA (H) shows the generation of mesopores with different sizes mainly in a range of 6-30 nm (Figure 21).

Table 4 shows the results obtained by mercury intrusions such as apparent density and particle porosity of the parent and hierarchical zeolites.

Table 4. Results obtained by mercury intrusion of the parent and hierarchical zeolites.

Sample	Apparent Density / $g \cdot mL^{-1}$	Particle Porosity / %
MOR P	1.719	72.59
MOR H	1.549	74.47
MFI P	1.793	63.12
MFI H	1.365	66.36
BEA P	1.458	67.33
BEA H	1.307	74.46

The decrease in apparent densities is caused by the extraction of silicon during the treatment, resulting in the mass loss of the particles, considering a constant volume (Table 4). On the other hand, the increase in particle porosity is due to the increase in the volume of mesopores. Therefore, the increased porosity in hierarchical zeolites is beneficial for the ketalization reaction by reducing the problems of diffusion and mass transfer.

4.2 Catalytic activity tests

Ketalization of glycerol with acetone to produce solketal was tested over parent and hierarchical zeolites of the MOR, MFI, and BEA framework. The catalytic activity tests are aimed at the performance of glycerol conversion and selectivity of solketal to choose the best catalyst for the synthesis. Figures 22 and 23 are represented the glycerol conversion over parent and hierarchical zeolites, respectively.

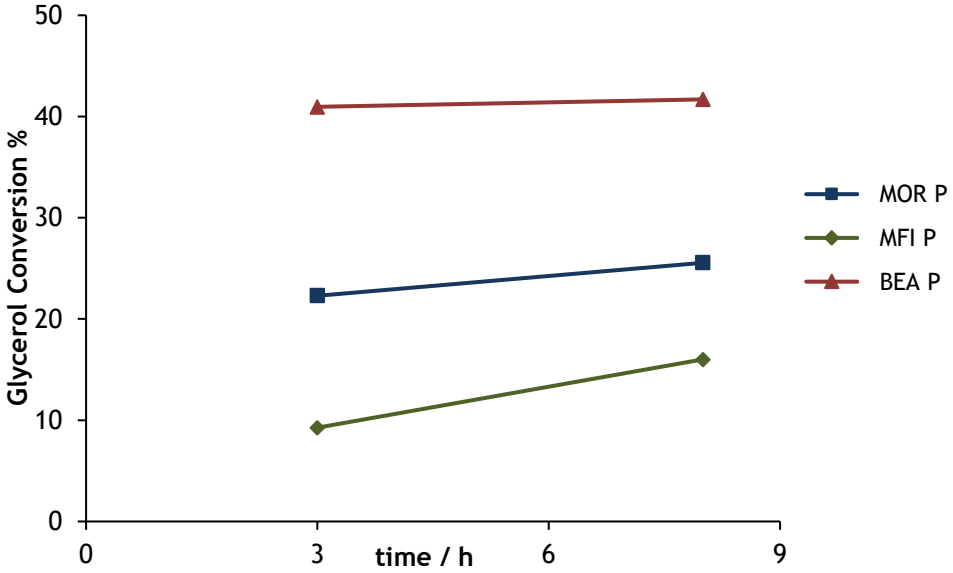

Figure 22. Glycerol conversion over parent zeolites MOR (P), MFI (P), and BEA (P).

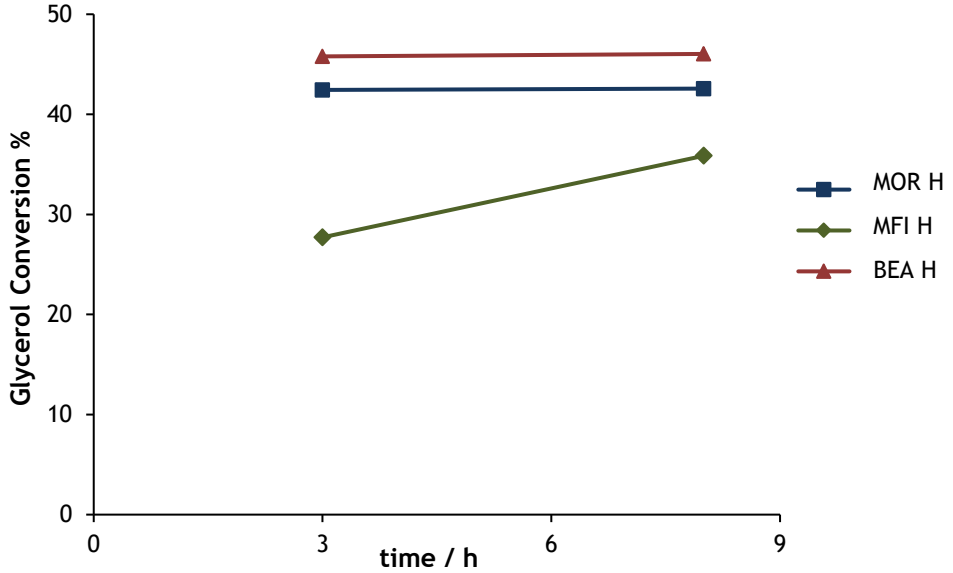

Figure 23. Glycerol conversion over hierarchical zeolites MOR (H), MFI (H), and BEA (H).

The MOR (P) and BEA (P) zeolites showed higher catalytic activity values when compared to MFI (P) which can be explained by the existence of larger pore size (Figures 22 and 24). The lower catalytic activity of MFI (P) may be related to the fact that this material has smaller and narrower pores, causing diffusional limitations.

However, when subjected to demetallation treatment, MOR (H) and MFI (H) had a perceptible change in the glycerol conversion. The MOR (H) showed a noteworthy increase in glycerol conversion at the end of 3 h and 8 h, by 20 % and 17 %, respectively. Also, after the treatment, MFI (H) increased the glycerol conversion at the end of 3 h by 18 %, and after 8 h by 29 % (Figure 23) and that may be explained due to increased mesoporosity and probably the size of the pores which influenced the catalytic activity. However, the modification procedure did not change the glycerol conversion noticeably in BEA (H) which has a minor difference in percentage value. Figures 24 and 25 are represented the selectivity to solketal over parent and hierarchical zeolites, respectively.

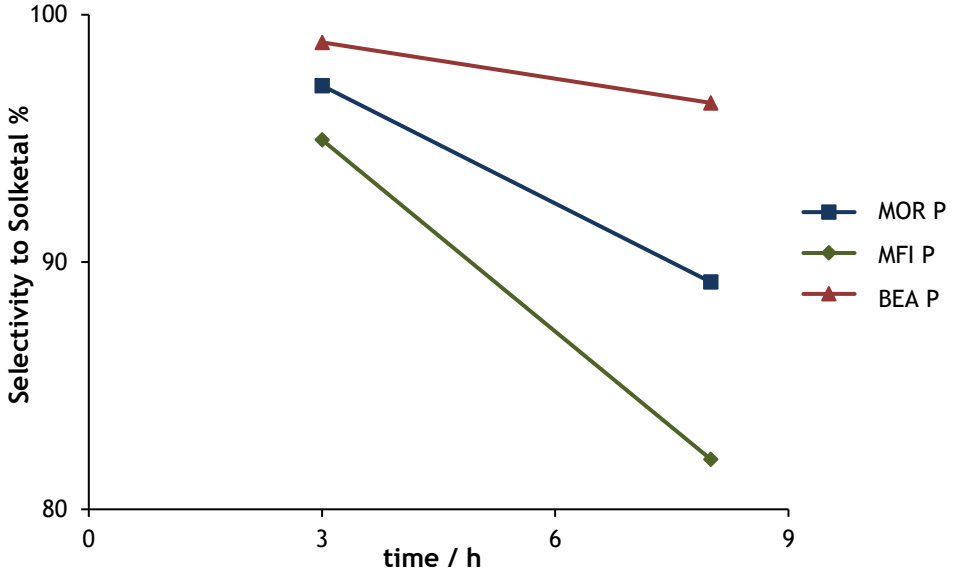

Figure 24. Selectivity to solketal over parent zeolites MOR (P), MFI (P), and BEA (P).

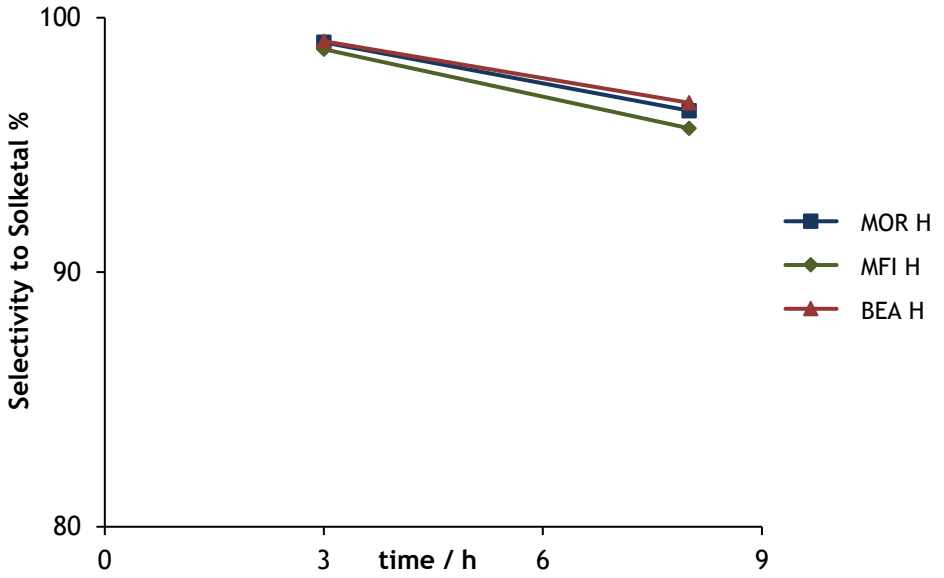

Figure 25. Selectivity to solketal over hierarchical zeolites MOR (H), MFI (H), and BEA(H).

Regarding the selectivity to solketal, the treatment of the zeolites results in an increase of selectivity, mainly in MFI (H) which increased by 3.82 % after 3 h. The increase in selectivity to solketal in MOR (H) was 1.93 %, whereas in BEA (H) it only increased by 0.19 %. Though, selectivity to solketal slightly changes to lowest values after 3 h.

In general, the catalytic activity of the parent zeolites was lower in contrast to the hierarchical zeolites because of the diffusion limitation, which after the treatments improved. However, MOR (H) and BEA (H) had better performance in glycerol conversion and selectivity to solketal, but MFI (H) had the most substantial increase in activity for ketalization reaction due to utilization of this treatment, to the increase of the mesoporosity and decrease in the diffusion limitation in this zeolite.

Also, the catalyst characterization of the zeolites after treatment in chapter 4.1 showed that the volume of mesopores in the MFI had the greatest increase, as well as the porosity. On the other hand, the duration of treatments for the MOR and BEA zeolite was longer due to the washing phase, and the loss of material, during the treatment was higher, which made MFI the best choice for the synthesis of solketal in the fixed bed column.

4.1 Catalyst Shaping

Mixtures of powder MFI Parent and hierarchical zeolites with different compositions were prepared as described in Section 3.3 until homogeneous pellets and with sufficient mechanical strength to be used as catalysts for packed a column for the synthesis of solketal were obtained. The fact of not knowing the exact composition of the paste, as well as the quantities of components for the optimal mixture, in order to obtain pellets with the required properties, made it necessary to teste various amounts of ultrapure water and binder in the parent zeolite. Table 5 shows the samples evaluated in MFI parent (P1-P4) and hierarchical (H1-H4) zeolites.

Table 5. Composition of tests of the extruded pellets.

Sample	Composition	Components of the mixture		
		Solid		Water / mL
		Zeolite/ g	Alumina / g	
P1	30 wt% Alumina + 0.65 mL H_20 per gram of solid	5.047	2.718	5.047
P2	30 wt% Alumina + 0.55 mL H_20 per gram of solid	5.120	2.194	4.023
P3	30 wt% Alumina + 0.45 mL H_20 per gram of solid	5.095	2.743	3.527
P4	30 wt% Alumina + 0.44 mL H_20 per gram of solid	15.00	6.430	9.429
H1	30 wt% Alumina + 0.44 mL H_20 per gram of solid	5.032	2.710	3.251
H2	30 wt% Alumina + 0.50 mL H_20 per gram of solid	2.036	0.873	1.454
H3	30 wt% Alumina + 0.59 mL H_20 per gram of solid	2.358	1.011	1.987
H4	30 wt% Alumina + 0.62 mL H_20 per gram of solid	2.171	0.930	1.861

The first experiments were performed from the MFI (P) to obtain the exact quantities of water and binder of the mixture to be posteriorly extruded. Figures 26, 27, 28, and 29 are represented the appearances of the paste and the extrudates obtained with the parent zeolite.

Sample P1 presented a wet texture and therefore was not extruded, because it was not the expected texture (Figure 26). The amount of water was reduced in sample P2, and the paste conferred a little bit of wet texture and when extruded a spaghetti/plasticine appearance was obtained. Besides that, there was an aggregation of the paste on the screw and die of the extruder, causing difficulty in the extrusion of the material. Despite that, the extrudates were manually cut into pellets and allowed to dry, and when placed in the spheronizer, they agglomerated (Figure 27).

Figure 26. Sample P1 composed with 30 wt% of alumina and 0.65 mL H_20 per gram of solid.

Figure 27. Sample P2 composed with 30 wt% of alumina and 0.55 mL H_20 per gram of solid.

The amount of water was reduced again in sample P3, and pellets were obtained with a texture similar to the expected, not so wet, and not so dry. After extrusion, the extrudates were manually cut into pellets, and after dried, they chipped (Figure 28). Therefore, the amount of water was reduced again in sample P4, and the paste had the desired appearance.

After extrusion, the extrudates were manually cut into pellets, after the spheronization and drying(calcination) they showed strong resistance (Figure 29).

It is verified that the optimal composition of the mixture for the production of pellets using the MFI (P), with mechanical resistance was 30 wt% alumina and 0.44 mL H_20 per gram of solid.

Figure 28. Sample P3 composed with 30 wt% of alumina and 0.45 mL H_20 per gram of solid.

Figure 29. Sample P4 composed with 30 wt% of alumina and 0.44 mL H_20 per gram of solid.

MFI (H) zeolites were tested with the same composition of the parent zeolite: 30 wt% alumina and 0.44 mL H_20 per gram of solid, to obtain the pellets and it was verified that the behavior of the material was different. It was observed that the appearance of the paste was much drier (Figure 30a) compared to the texture of the paste using the MFI (P), and upon extrusion, the extruder overheated, and no pellets were formed. This is due to the fact that in the treatments, zeolites with greater mesoporosity were created, and when adding water, they

adsorb more. It was necessary to take this into account and increase the amount of water in the mixture.

The amount of water was increased in sample H2 and there was no great difference, so the extrusion of the pellets was not tested. The amount of water was increased again for samples H3 and H4, where it was found that a small amount of water could have a significant impact on changing the texture of the paste. Figures 30b and 30c corresponds to samples H3 and H4, respectively.

Figure 30. Appearance of paste of MFI (H) zeolite (a) too dry, (b) optimal, and (c) too wet.

After extrusion, the extrudates from sample H4 (Figure 30c) had a texture identical to sample P2, so it was discarded. In sample H3 (Figure 30b), the appearance of the paste was identical to sample P4 and the extrudates were also manually cut into pellets. After the spheronization and drying (calcination) they showed strong resistance. The pellets obtained are shown in Figure 31. The optimal composition of the mixture for the production of pellets using the MFI (H) was 30 wt% alumina and 0.59 mL H_20 per gram of solid.

Figure 31. Pellets of MFI (H).

In order to pack the fixed bed for the synthesis of solketal, it was necessary to produce around 20 g of pellets. Additional batches were then prepared. In the production of more pellets with the same composition, it was found that another factor that had an impact on the

composition of the mixture was the humidity because depending on the day, more/less water was needed. Therefore, this had a great influence on the production of pellets. For that reason, in some of the mixtures, the appearance had to be considered and more/less water had to be added to the amount of water previously tested, based on optimal appearance in Figure 30b.

4.2 Solketal production in a fixed bed column

The dynamic behavior of MFI (H) was evaluated for the production of solketal, as the desired product. Figure 32 shows the fixed bed column packed with the pellets.

Figure 32. Packed column with pellets of MFI (H).

The outlet stream concentration was recorded for up to 40 minutes and is represented in Figure 33. The results demonstrate that the fixed bed adsorptive reactor packed with pellets of MFI (H) was capable of converting the glycerol and acetone into solketal product.

The use of adsorptive pellets is intended to retain water as a reaction product by being adsorbed, contributing to the production of solketal with the separation of these two. Furthermore, from the outlet data concentration, the solketal has been identified firstly at the outlet at 11 min, and water was the last species to be detected at the outlet at 13 min.

Besides, the fact the ketalization reaction has a stoichiometric molar ratio of 1:1 to acetone and glycerol, the concentrations of reactants and products tend to equivalent values, respectively.

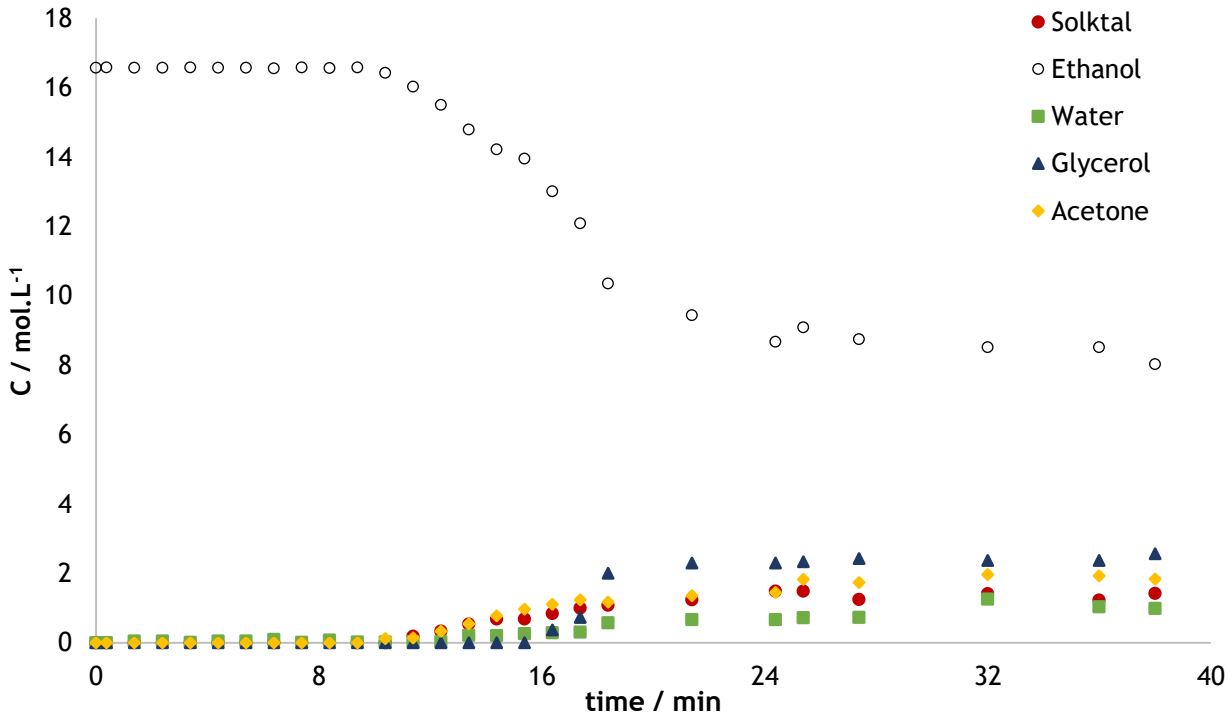

Figure 33. Outlet concentration of reactants and products with the solvent outlet concentration for the synthesis of solketal in fixed-bed reactor at 323K.

5 Assessment of the work done

5.1 Objectives Achieved

The main objectives achieved in this work were:

1. Preparation of three types of hierarchical zeolites with demetallation treatment
2. Characterization of the hierarchical zeolites with the technique of X-ray diffraction, nitrogen adsorption, and mercury intrusion porosimetry;
3. Evaluation of the hierarchical zeolites in catalytic tests with results of glycerol conversion and selectivity to solketal;
4. Shaping the hierarchical zeolite with greater increase on catalytic tests;
5. Solketal production in a fixed bed column packed with pellets.

5.2 Limitations and Future Work

One of the limitations of the work was the washing time of the zeolites, which was different between them and made the treatment time-consuming. In addition, constant breakdowns in the department's centrifuges caused delays in the work plan.

It is also interesting to carry out further characterization of the catalyst with other techniques, such as Scanning Electron Microscopy (SEM), to know the impact of the treatment on the surface of zeolites, from images of the morphology of the materials.

On the other hand, for future work the formulation/composition of the mixture for the pellets shaping must be improved, and it would be important after the extrusion, to repeat the catalytic tests to evaluate the catalytic activity. Mechanical strength tests and catalyst characterization of the pellets would also be important to evaluate the impact on the extruded.

The experiments in the fixed-bed column require more tests to obtain equilibrium and kinetic parameters. Also, preliminary tests to assesses the impact of mass transfer resistances must be done.

5.3 Final Assessment

The final evaluation of this work is positive, despite not having fulfilled all the objectives due to time constraints. The development of this dissertation helped me to have a broad view of the work of an investigator and was an agreeable challenge.

6 References

1. Pagliaro , M. and M. Rossi *Glycerol: Properties and Production*, in *The Future of Glycerol: New Usages for a Versatile Raw Material*. 2008, The Royal Society of Chemistry. p. 1-17.
2. Quispe, C.A.G., C.J.R. Coronado, and J.A. Carvalho Jr, *Glycerol: Production, consumption, prices, characterization and new trends in combustion*. Renewable and Sustainable Energy Reviews, 2013. **27**: p. 475-493.
3. Nanda, M.R., Y. Zhang, Z. Yuan, W. Qin, H.S. Ghaziaskar, and C. Xu, *Catalytic conversion of glycerol for sustainable production of solketal as a fuel additive: A review*. Renewable and Sustainable Energy Reviews, 2016. **56**: p. 1022-1031.
4. Checa, M., S. Nogales-Delgado, V. Montes, and J.M. Encinar, *Recent Advances in Glycerol Catalytic Valorization: A Review*. Catalysts, 2020. **10**(11): p. 1279.
5. Morrison, L.R., *Glycerol*, in *Kirk-Othmer Encyclopedia of Chemical Technology*. 2000.
6. Amaral, P.F.F., T.F. Ferreira, G.C. Fontes, and M.A.Z. Coelho, *Glycerol valorization: New biotechnological routes*. Food and Bioproducts Processing, 2009. **87**(3): p. 179-186.
7. *IEA, Global Energy Review: CO2 Emissions in 2021*. 2022; Available from: https://www.iea.org/reports/global-energy-review-co2-emissions-in-2021-2. Accessed on 26 March 2022.
8. *IEA , Tracking Transport 2021*. 2022. Available from: https://www.iea.org/reports/tracking-transport-2021. Accessed on 26 March 2022.
9. Jeswani, H.K., A. Chilvers, and A. Azapagic, *Environmental sustainability of biofuels: a review*. Proceedings. Mathematical, physical, and engineering sciences, 2020. **476**(2243): p. 20200351-20200351.
10. Chilakamarry, C.R., A.M.M. Sakinah, A.W. Zularisam, and A. Pandey, *Glycerol waste to value added products and its potential applications*. Systems Microbiology and Biomanufacturing, 2021. **1**(4): p. 378-396.
11. Rouhany, M. and H. Montgomery, *Global Biodiesel Production: The State of the Art and Impact on Climate Change*, in *Biodiesel: From Production to Combustion*, M. Tabatabaei and M. Aghbashlo, Editors. 2019, Springer International Publishing: Cham. p. 1-14.
12. Zahid, I., M. Ayoub, B.B. Abdullah, A. Mukhtar, S. Saqib, S. Rafiq, S. Ullah, A.G. Al-Sehemi, S. Farrukh, and M. Danish, *Glycerol Conversion to Solketal: Catalyst and Reactor Design, and Factors Affecting the Yield*. ChemBioEng Reviews, 2021. **8**(3): p. 227-238.
13. Rossa, V., Y.d.S.P. Pessanha, G.C. Díaz, L.D.T. Câmara, S.B.C. Pergher, and D.A.G. Aranda, *Reaction Kinetic Study of Solketal Production from Glycerol Ketalization with Acetone*. Industrial & Engineering Chemistry Research, 2017. **56**(2): p. 479-488.
14. Kaur, J., A.K. Sarma, M.K. Jha, and P. Gera, *Valorisation of crude glycerol to value-added products: Perspectives of process technology, economics and environmental issues*. Biotechnology Reports, 2020. **27**: p. e00487.
15. Datta, I., A. Ghosh, A. Acharjee, A. Rakshit, and B. Saha, *Overview on biodiesel market*. 2021. **59**: p. 271-284.
16. Alsaadi, L., V. Eze, and A. Harvey, *Techno-Economic Analysis of Glycerol Valorization via Catalytic Applications of Sulphonic Acid-Functionalized Copolymer Beads*. Frontiers in Chemistry, 2020. **7**.

17. Kosamia, N.M., M. Samavi, B.K. Uprety, and S.K. Rakshit, *Valorization of Biodiesel Byproduct Crude Glycerol for the Production of Bioenergy and Biochemicals*. Catalysts, 2020. **10**(6).

18. Trifoi, A.R., P.Ş. Agachi, and T. Pap, *Glycerol acetals and ketals as possible diesel additives. A review of their synthesis protocols.* Renewable and Sustainable Energy Reviews, 2016. **62**: p. 804-814.

19. Kaur, J., P. Gera, M. Jha, and A. Sarma, *A Study on Conversion of Glycerol into Solketal Using Rice Husk-Derived Catalyst*. 2020. p. 599-606.

20. Khodadadi, M.R., J. Thiel, R.S. Varma, and C. Len, *Innovative continuous synthesis of solketal*. Journal of Flow Chemistry, 2021. **11**(4): p. 725-735.

21. Corrêa, I., R.P.V. Faria, and A.E. Rodrigues, *Continuous Valorization of Glycerol into Solketal: Recent Advances on Catalysts, Processes, and Industrial Perspectives*. Sustainable Chemistry, 2021. **2**(2).

22. Vannucci, J.A., M.N. Gatti, N. Cardaci, and N.N. Nichio, *Economic feasibility of a solketal production process from glycerol at small industrial scale*. Renewable Energy, 2022. **190**: p. 540-547.

23. Zahid, I., M. Ayoub, B.B. Abdullah, M.H. Nazir, M. Ameen, Zulqarnain, M.H. Mohd Yusoff, A. Inayat, and M. Danish, *Production of Fuel Additive Solketal via Catalytic Conversion of Biodiesel-Derived Glycerol*. Industrial & Engineering Chemistry Research, 2020. **59**(48): p. 20961-20978.

24. Kowalska-Kuś, J., A. Held, M. Frankowski, and K. Nowinska, *Solketal formation from glycerol and acetone over hierarchical zeolites of different structure as catalysts*. Journal of Molecular Catalysis A: Chemical, 2016. **426**.

25. Kowalska-Kuś, J., A. Held, and K. Nowińska, *Solketal Formation in a Continuous Flow Process over Hierarchical Zeolites*. ChemCatChem, 2020. **12**(2): p. 510-519.

26. Chen, L.-H., M.-H. Sun, Z. Wang, W. Yang, Z. Xie, and B.-L. Su, *Hierarchically Structured Zeolites: From Design to Application*. Chemical Reviews, 2020. **120**(20): p. 11194-11294.

27. Bai, R., Y. Song, Y. Li, and J. Yu, *Creating Hierarchical Pores in Zeolite Catalysts*. Trends in Chemistry, 2019. **1**(6): p. 601-611.

28. Valtchev, V. and S. Mintova, *Hierarchical zeolites*. MRS Bulletin, 2016. **41**(9): p. 689-693.

29. Dusselier, M. and M.E. Davis, *Small-Pore Zeolites: Synthesis and Catalysis*. Chemical Reviews, 2018. **118**(11): p. 5265-5329.

30. Holm, M.S., E. Taarning, K. Egeblad, and C.H. Christensen, *Catalysis with hierarchical zeolites*. Catalysis Today, 2011. **168**(1): p. 3-16.

31. Talebian-Kiakalaieh, A. and S. Tarighi, *Hierarchical faujasite zeolite-supported heteropoly acid catalyst for acetalization of crude-glycerol to fuel additives*. Journal of Industrial and Engineering Chemistry, 2019. **79**: p. 452-464.

32. Khan, W., X. Jia, Z. Wu, J. Choi, and A.C.K. Yip, *Incorporating Hierarchy into Conventional Zeolites for Catalytic Biomass Conversions: A Review*. Catalysts, 2019. **9**(2).

33. Feliczak-Guzik, A., *Hierarchical zeolites: Synthesis and catalytic properties*. Microporous and Mesoporous Materials, 2018. **259**: p. 33-45.

34. Srivastava, R., *Synthesis and applications of ordered and disordered mesoporous zeolites: Present and future prospective*. Catalysis Today, 2018. **309**: p. 172-188.

35. *IZA Structure Commission*. 30/03/2022; Available from: http://www.iza-structure.org/. Accessed on 5 april 2022

36. Hartmann, M., A.G. Machoke, and W. Schwieger, *Catalytic test reactions for the evaluation of hierarchical zeolites*. Chemical Society Reviews, 2016. **45**(12): p. 3313-3330.

37. Castro, B., *Development of hierarchical zeolites*. Thesis, 2020, FEUP. p. 14-16.

38. Selva, T.M.G., J.S.G. Selva, and R.B. Prata, *Sensing Materials: Diamond-Based Materials*, in *Reference Module in Biomedical Sciences*. 2021, Elsevier.

39. Bunaciu, A.A., E.g. Udriştioiu, and H.Y. Aboul-Enein, *X-Ray Diffraction: Instrumentation and Applications*. Critical Reviews in Analytical Chemistry, 2015. **45**(4): p. 289-299.

40. Liu, P.S. and G.F. Chen, *Chapter Nine - Characterization Methods: Basic Factors*, in *Porous Materials*, P.S. Liu and G.F. Chen, Editors. 2014, Butterworth-Heinemann: Boston. p. 411-492.

41. Sidiq, A., R.J. Gravina, S. Setunge, and F. Giustozzi, *High-efficiency techniques and micro-structural parameters to evaluate concrete self-healing using X-ray tomography and Mercury Intrusion Porosimetry: A review*. Construction and Building Materials, 2020. **252**: p. 119030.

42. Bingre, R., B. Louis, and P. Nguyen, *An Overview on Zeolite Shaping Technology and Solutions to Overcome Diffusion Limitations*. Catalysts, 2018. **8**(4): p. 163.

43. Rioland, G., T.J. Daou, D. Faye, and J. Patarin, *A new generation of MFI-type zeolite pellets with very high mechanical performance for space decontamination*. Microporous and Mesoporous Materials, 2016. **221**: p. 167-174.

44. *Caleva*. Available from: https://www.caleva.com/products/multi-lab-for-pellet-research-and-development/. Accessed on 15 june 2022.

45. Xu, L., Y. Zhang, J. Ding, Y. Liu, Y. Shi, Y. Li, Y. Dang, N.-C. Cheng, and G. Anfu, *Pore Structure and Fractal Characteristics of Different Shale Lithofacies in the Dalong Formation in the Western Area of the Lower Yangtze Platform*. Minerals, 2020. **10**: p. 72.

7 Conclusion

The development of hierarchical zeolites in shaped form, after the demetallation treatment of parent zeolites, to be used in a packed fixed-bed column for further experiments in the synthesis of solketal, was the main objective of this work.

The characterization results show that the treatments had no impact on the crystallinity of the zeolites since in X-Ray diffraction spectra show the same characteristic peaks as the original material and no additional peaks were detected. Even though the intensity of the different peaks was different. On the other hand, from the nitrogen adsorption data, the formation of mesopores was verified. The impact of the treatment formed wedge-shaped pores in all structures, causing an increase in the adsorbed volume of N_2. The increased external surface area and mesoporous volume in the structures demonstrated the effectiveness of the treatment. Nonetheless, the higher increase in the formation of the mesoporous structure was more evident in the hierarchical MFI zeolite, with an increase in adsorbed volume compared to the parent.

An increase in porosity was also observed after the treatments, as a result of the increase in the volume of mesopores, which is beneficial for the ketalization reaction by reducing the problems of diffusion and mass transfer.

The catalytic activity of the zeolites also improved after the treatment in which the MFI (H) had the most significant increase of 29% after 8h on glycerol conversion and 3.82% after 3h at selectivity to solketal, comparatively to other hierarchical zeolites. MOR (H) and HBEA (H) had better performance in glycerol conversion and selectivity to solketal. Hierarchical MFI zeolite was selected for the synthesis of solketal in the fixed bed column due to the highest improvement due to the treatment but also the duration of the treatment which is longer in the MOR and BEA zeolite. For this, it was necessary to form pellets from extrusion, in which several tests were needed from the parent zeolite powder to obtain the best composition of the mixture for the pellets. The optimal composition of the mixture to produce pellets found was 30 wt% alumina and 0.59 mL H_20 per gram of solid.

The evaluation of production of solketal in a fixed-bed column packed with MFI(H) pellets was tested and it was demonstrated that the conversion of glycerol was possible at 323 K.

Annex A - Gas Chromatograph calibration for catalytic activity tests

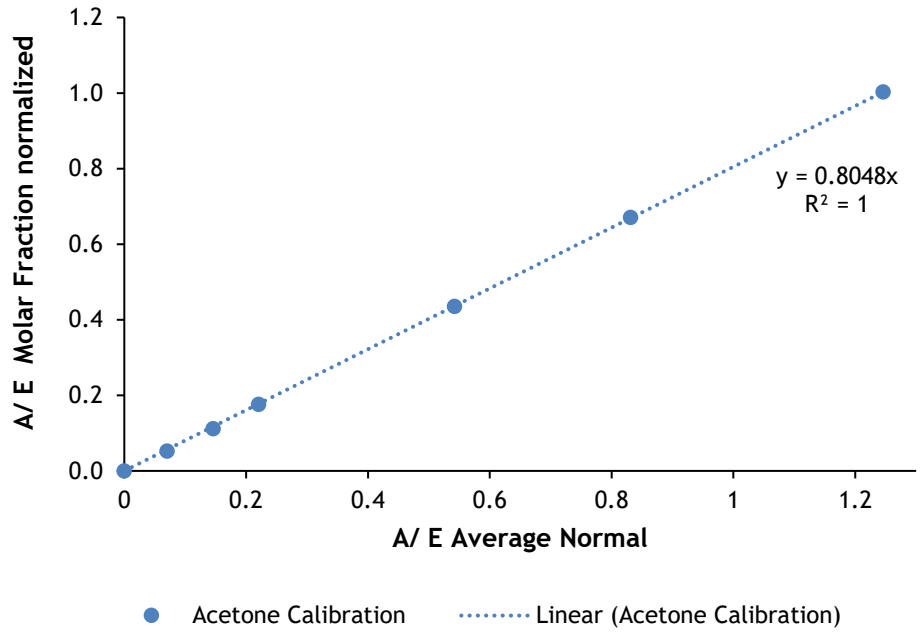

Figure 34. Acetone Calibration for the catalytic tests.

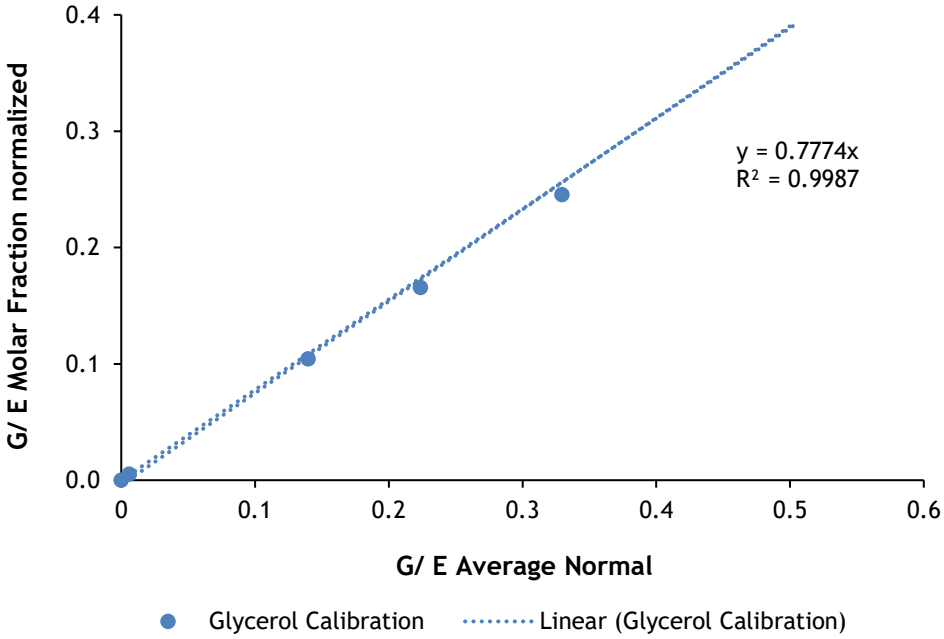

Figure 35. Glycerol Calibration for the catalytic tests.

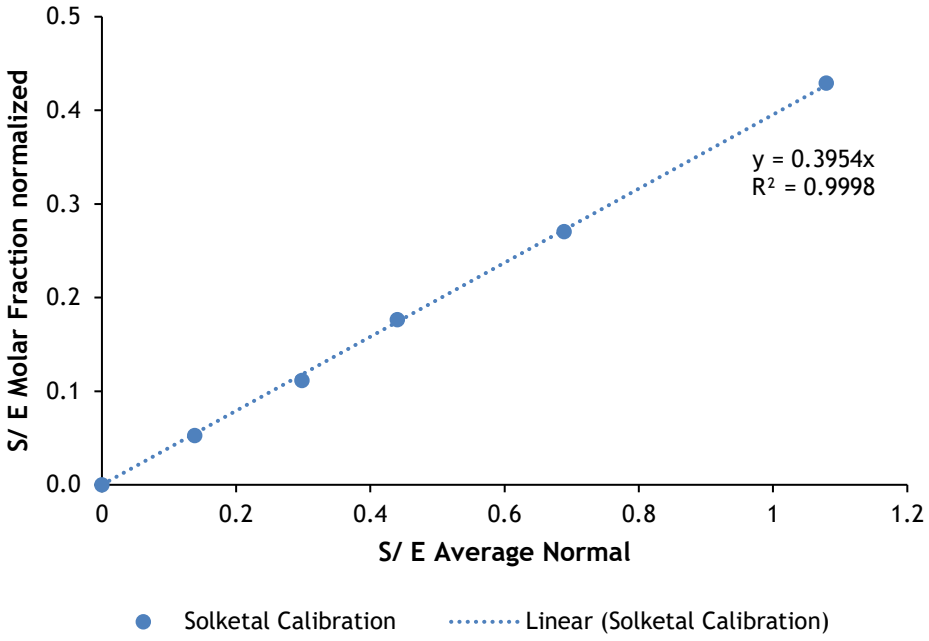

Figure 36. Solketal Calibration for the catalytic tests.

Annex B - Gas Chromatograph calibration for solketal production

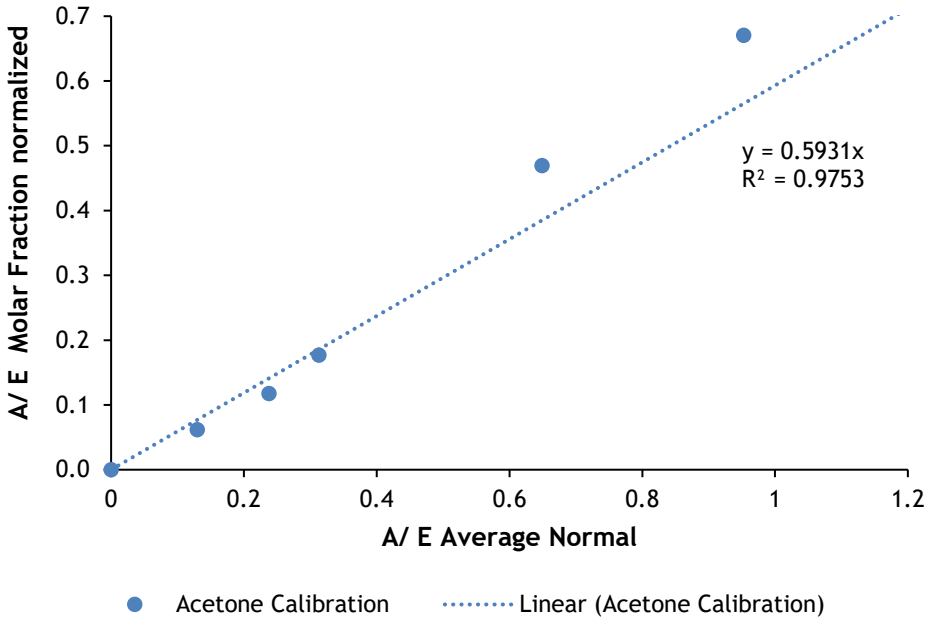

Figure 37. Acetone Calibration for the solketal production.

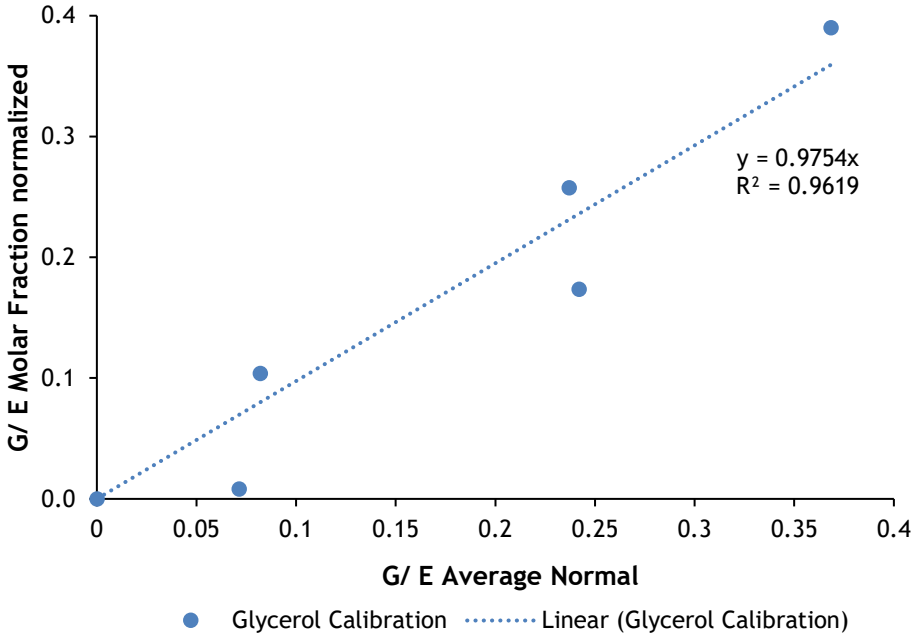

Figure 38. Glycerol Calibration for the solketal production.

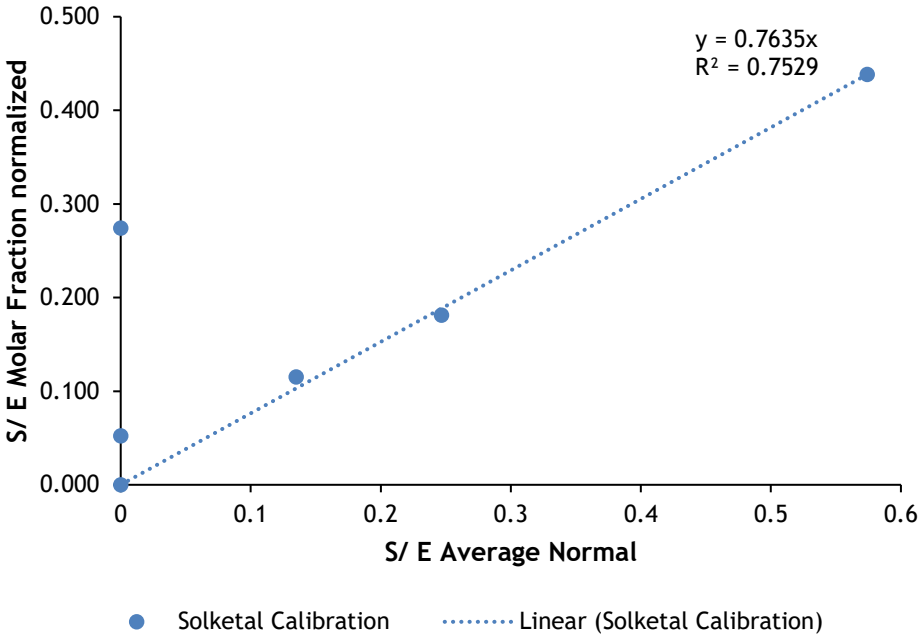

Figure 39. *Solketal* Calibration for the solketal production.

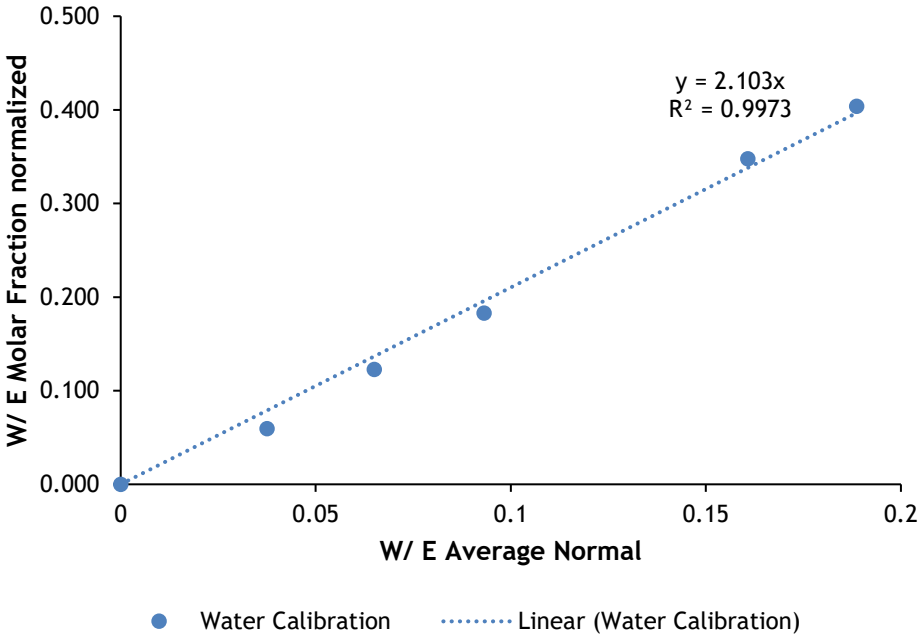

Figure 40. Water Calibration for the solketal production.